

AD-A049 933

AIR FORCE INST OF TECH WRIGHT-PATTERSON AFB OHIO
APPROXIMATE SOLUTIONS TO THE RADIATIVE TRANSFER EQUATION USING --ETC(U)

F/0 4/1

AUG 77 P J BRESLIN

UNCLASSIFIED

AFIT-CI-78-25

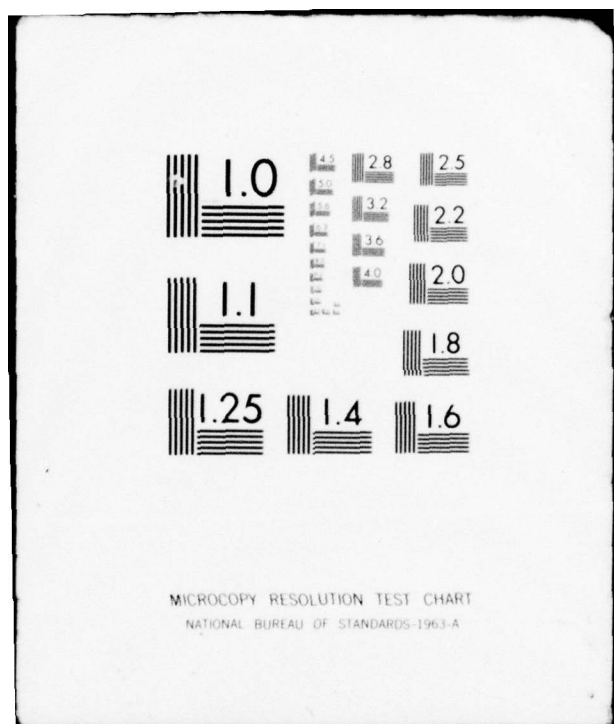
NL

| OF |
AD
AD49933
FIE

\emptyset



END
DATE
FILED
3-78
DDC



AD No. 1
FILE COPY

AD A049933

78-252

(1)

(6) APPROXIMATE SOLUTIONS TO THE RADIATIVE TRANSFER
EQUATION USING THE ELSASSER SCHEME

(10) by
Paul Joseph Breslin

(12) 65 p.

(9) Master's thesis,

A thesis submitted to the faculty of the
University of Utah in partial fulfillment of the requirements
for the degree of

(14) AFIT-CI-78-25

Master of Science

DDC
RECEIVED
FEB 14 1978
RECEIVED
D

Department of Meteorology

University of Utah

(11) August 1977

012300

DISTRIBUTION STATEMENT A

Approved for public release;
Distribution Unlimited

UNCLASSIFIED

SECURITY CLASSIFICATION OF THIS PAGE (When Data Entered)

REPORT DOCUMENTATION PAGE		READ INSTRUCTIONS BEFORE COMPLETING FORM
1. REPORT NUMBER CI 78-25	2. GOVT ACCESSION NO.	3. RECIPIENT'S CATALOG NUMBER
4. TITLE (and Subtitle) Approximate Solutions to the Radiative Transfer Equation Using the Elsasser Scheme		5. TYPE OF REPORT & PERIOD COVERED Thesis
7. AUTHOR(s) Captain Paul J. Breslin		6. PERFORMING ORG. REPORT NUMBER
9. PERFORMING ORGANIZATION NAME AND ADDRESS AFIT/CI Student at the University of Utah, Salt Lake City UT		10. PROGRAM ELEMENT, PROJECT, TASK AREA & WORK UNIT NUMBERS
11. CONTROLLING OFFICE NAME AND ADDRESS AFIT/CI WPAFB OH 45433		12. REPORT DATE August 1977
14. MONITORING AGENCY NAME & ADDRESS(if different from Controlling Office)		13. NUMBER OF PAGES 57 Pages
16. DISTRIBUTION STATEMENT (of this Report) Approved for Public Release; Distribution Unlimited		15. SECURITY CLASS. (of this report) Unclassified
17. DISTRIBUTION STATEMENT (of the abstract entered in Block 20, if different from Report)		15a. DECLASSIFICATION/DOWNGRADING SCHEDULE
18. SUPPLEMENTARY NOTES For James E. Sharpen JERAL F. GUESS, Captain, USAF Director of Information, AFIT APPROVED FOR PUBLIC RELEASE AFR 190-17. MSgt, USAF Deputy Director of Information		
19. KEY WORDS (Continue on reverse side if necessary and identify by block number)		
20. ABSTRACT (Continue on reverse side if necessary and identify by block number)		

ACCESSION for	
DIS	White <input checked="" type="checkbox"/>
DOC	Soft Edition <input type="checkbox"/>
ANNOUNCED	
JUSTIFICATION	
DISTRIBUTION/AVAILABILITY CODES	
Dist.	AVAIL. and/or SPECIAL
A	

THE UNIVERSITY OF UTAH GRADUATE SCHOOL

SUPERVISORY COMMITTEE APPROVAL

of a thesis submitted by

Paul Joseph Breslin

I have read this thesis and have found it to be of satisfactory quality for a master's degree.

6/17/77
Date

Wilford G. Zdunkowski
Wilford G. Zdunkowski
Chairman, Supervisory Committee

I have read this thesis and have found it to be of satisfactory quality for a master's degree.

6/17/77
Date

Kuo-Nan Liou
Kuo-Nan Liou
Member, Supervisory Committee

I have read this thesis and have found it to be of satisfactory quality for a master's degree.

6/17/77
Date

Jan Paegle
Jan Paegle
Member, Supervisory Committee

THE UNIVERSITY OF UTAH GRADUATE SCHOOL

FINAL READING APPROVAL

To the Graduate Council of The University of Utah:

I have read the thesis of Paul Joseph Breslin in its final form and have found that (1) its format, citations, and bibliographic style are consistent and acceptable; (2) its illustrative materials including figures, tables, and charts are in place; and (3) the final manuscript is satisfactory to the Supervisory Committee and is ready for submission to the Graduate School.

17 June 1977

Date

Wilford G. Zdunkowski

Wilford G. Zdunkowski
Member, Supervisory Committee

Approved for the Major Department

S. K. Kao

S. K. Kao
Chairman/Dean

Approved for the Graduate Council

Sterling M. McMurrin
Dean of The Graduate School

ABSTRACT

In a recent paper Charlock, Herman and Zdunkowski (1976) disagree on how best to apply the Radiative Transfer Equation (RTE) in the construction of Elsasser type radiation tables. The two proposed approximate solutions are analyzed and compared against a quasi-exact solution. Infrared fluxes and cooling rates are calculated for part of the $6.3 \mu\text{m}$ water vapor band for two model atmospheres. It is found that the Zdunkowski (Z) approximation yields more accurate downward fluxes, while the Charlock-Herman (CH) approximation, in general, results in more accurate upward fluxes. For the two model atmospheres studied the cooling rates for the Z approximation are usually of better quality than those due to the CH solution, unless the divergence of the net flux is extremely small.

ACKNOWLEDGMENTS

The author would like to express his appreciation to Dr. Jan Paegle and Dr. Kuo-Nan Liou for serving on the supervisory committee and providing patient guidance during the past year. Sincere thanks are also due Dr. Wilford G. Zdunkowski for serving as committee chairman, without whose encouragement and valuable advice this work would not have been completed. The help provided by Dr. Elford G. Astling in selecting a representative model atmosphere is greatly appreciated.

TABLE OF CONTENTS

	<u>Page</u>
ABSTRACT	iv
ACKNOWLEDGMENTS	v
LIST OF FIGURES	vii
LIST OF TABLES	viii
SECTION	
I. INTRODUCTION	1
II. DATA AND ANALYSIS	3
2.1 Symbols	3
2.2 The Model Equations	4
2.3 The Elsasser Scheme	4
2.4 The Charlock-Herman Approximation (CH, 1976) .	9
2.5 The Approximation by Zdunkowski, Barth and Lombardo (1966)	11
2.6 Numerical Treatment	13
2.7 Properties of Approximations	15
III. DISCUSSION AND RESULTS	21
3.1 Atmospheric Models	21
3.2 Flux Transmission Function	21
3.3 Infrared Fluxes	22
3.4 Cooling Rates	31
IV. CONCLUSION	34
APPENDIX A: RADIATIVE TRANSFER EQUATION	35
APPENDIX B: LISTINGS OF COMPUTER PROGRAMS	42
REFERENCES	56
VITA	57

LIST OF FIGURES

<u>Figure No.</u>		<u>Page</u>
1	Schematic representation of flux integration limits	5
2	Generalized absorption coefficient for 6.3 μm water-vapor band for various temperatures ($^{\circ}\text{C}$) . .	6
3	Model Atmospheres I and II	16
4	Schematic representation of optical path for flux integration	38

LIST OF TABLES

<u>Table No.</u>		<u>Page</u>
1	Selected Values of Flux Transmission for Interpolant and for EC Data as a Function of $x = \log_{10}$ (optical path)	23
2	Upward Fluxes and Approximate Solution Errors at Selected Levels for Model I	24
3	Downward Fluxes and Approximate Solution Errors at Selected Levels for Model I	25
4	Net Fluxes and Approximate Solution Errors at Selected Levels for Model I	26
5	Upward Fluxes and Approximate Solution Errors at Selected Levels for Model II	28
6	Downward Fluxes and Approximate Solution Errors at Selected Levels in Model II	29
7	Net Fluxes and Approximate Solution Errors at Selected Levels in Model II	30
8	Cooling Rates for Model I at Selected Layers . . .	32
9	Cooling Rates for Model II at Selected Layers . . .	33

I. INTRODUCTION

The transfer of Infrared Radiation in the earth's atmosphere is of great interest to meteorologists. Over the years different mathematical models have been exploited with varying degrees of success. All of these are special cases of the fundamental Radiative Transfer Equation (RTE), whose solution is known in principle. However, there are many difficulties in their practical application to the atmosphere. Hence, various approximations are proposed to simplify the computation of atmospheric radiative fluxes and attendant cooling rates.

In 1966 Zdunkowski, Barth and Lombardo and Zdunkowski (1971), hereafter referred to as Z, proposed an approximate solution to the RTE based upon the original work of Elsasser and Culbertson (1960), hereafter referred to as EC. In 1976, Charlock and Herman, hereafter referred to as CH, claim to have obtained the "correct expression" for infrared radiative transfer and reject Z's approximation as incorrect. However, Z (Charlock, Herman, Zdunkowski, 1976) points out that their expressions are merely approximations and it is improper, a priori, to dismiss one approximation in favor of another.

→ The purpose of this study is to analyze and compare the atmospheric radiative fluxes and cooling rates resulting from ~~the~~ two approximations, ~~mentioned above~~ As a norm for the comparison, a quasi-exact solution is also applied. This is accomplished by using

next
page

cont. the EC formulation of the generalized absorption coefficient. Calculations are carried out for two model atmospheres for part of the 6.3 micron water vapor band.

Initially, it was planned to check the quality of the two approximations against measurements, but it is believed that the computational type of comparison is more useful and definitive.

It is found that the Z approximation is more accurate for the downward fluxes and the CH approximation is more accurate for the upward fluxes. For the model atmospheres studied the cooling rate errors are usually smaller for the Z approximation, unless the divergence of the net flux is extremely small.

15

II. DATA AND ANALYSIS

2.1 Symbols

To guarantee a consistent notation it is useful to first define the following symbols:

B_v	monochromatic hemispheric black body flux at wavenumber v ; a subscript G refers to the ground.
$Z', P, T - T_0, P_0$	height, temperature, pressure; subscript "0" refers to standard values.
ρ_v	absorber density.
$u = \int \rho_v dz'$	absorber mass in a vertical column of air $[\text{gm cm}^{-2}]$.
u^*	reduced absorber mass.
K_v	absorption coefficient.
L_v, L_0	generalized absorption coefficient; $L_0 = L_v(T_0)$
$\tau = \int K_v(u)du$	optical pathlength (not to be confused with transmission function).
$\tau_{F,v}$	^{monochromatic} flux transmission function.
F_v^{\downarrow}	downward monochromatic flux.
F_v^{\uparrow}	upward monochromatic flux.
t	time.

2.2 The Model Equations

For a plane parallel, horizontally homogeneous, non-scattering atmosphere an exact solution to the RTE exists. Assuming the absence of downward radiation at the top of the atmosphere, the solution to the RTE for downward monochromatic flux (Figure 1) at the reference level, u_0 , is given by (See Appendix I)

$$F_v^{\downarrow}(u_0) = \int_0^{u_0} B_v(u) \frac{d}{du} \left\{ \tau_F \left(\int_u^{u_0} K_v(u_1) du_1 \right) \right\} du \quad (1)$$

The monochromatic upward flux at the reference level is expressed as

$$F_v^{\uparrow}(u_0) = B_{v,G} \tau_F \left(\int_{u_0}^U K_v(u_1) du_1 \right) - \int_{u_0}^U B_v(u) \frac{d}{du} \left\{ \tau_F \left(\int_{u_0}^u K_v(u_1) du_1 \right) \right\} du \quad (2)$$

Note that the absorption coefficient, K_v , is a function of pressure and temperature.

2.3 The Elsasser Scheme

In order to facilitate flux calculations, EC replace the rapidly varying absorption coefficient, K_v , by an empirically determined, more slowly varying, generalized absorption coefficient, L_v . While K_v varies with pressure and temperature, L_v is assumed to depend only on temperature (Figure 2). The temperature dependence is given by

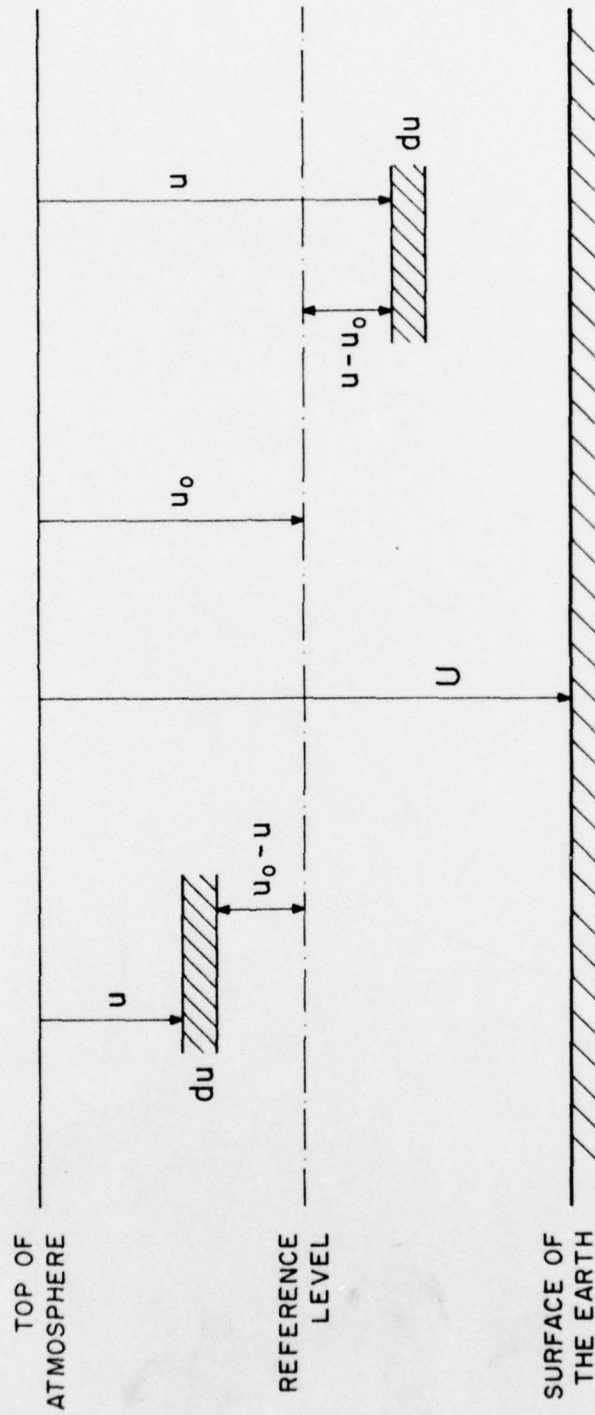


Figure 1. Schematic representation of flux integration limits.

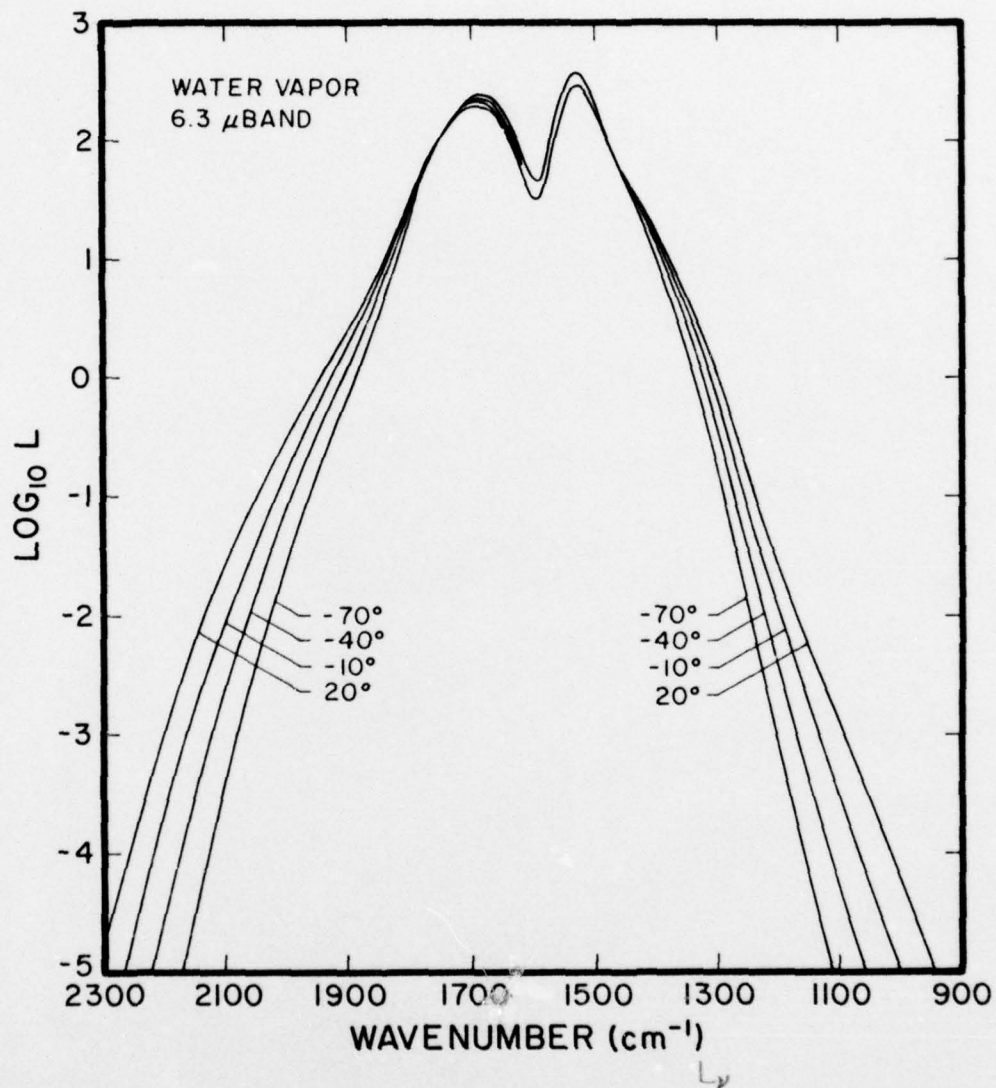


Figure 2. Generalized absorption coefficient for the $6.3 \mu\text{m}$ water vapor band for various temperatures ($^\circ\text{C}$).

EC (1960) as

$$\log_{10} L = \log_{10} L_0 - a \frac{(T_0 - T)}{T} (v - v_0)^2 + \log_{10} \frac{T_0}{T} \quad (3)$$

The quantities L_0 , v_0 and a are given by EC.

In view of the EC approximation, the pressure broadening effect on the absorption coefficient is included by defining the reduced absorbing mass, i.e.,

$$du^* = \rho_v(z') \frac{P(z')}{P_0} \left(\frac{T_0}{T(z')} \right)^{1/2} dz' \quad (4)$$

Using Equations (3,4) the argument of the transmission function becomes

$$\begin{aligned} \int_z^{z''} K_v [P(z'), T(z')] \rho_v(z') dz' &= \int_u^{u_0} K_v [P(u_1), T(u_1)] du_1 \\ &= \int_z^{z''} L_v [T(z')] \rho_v(z') \frac{P(z')}{P_0} \left(\frac{T_0}{T(z')} \right)^{1/2} dz' \\ &= \int_{u^*}^{u_0} L_v (T(u_1^*)) du_1^* \end{aligned} \quad (5)$$

Substituting Equation (5) into Equation (1) and integrating by parts yields

$$F_v^+(u_0^*) \doteq \int_0^{u_0^*} B_v(u^*) \frac{d}{du^*} \tau_F \left(\int_{u^*}^{u_0^*} L_v(u_1^*) du_1^* \right) du^*$$

$$\begin{aligned}
 &= B_v(T(u_0^*)) - B_v(T(u^*=0)) \tau_F \left(\int_0^{u_0^*} L_v(u_1^*) du_1^* \right) \\
 &\quad - \int_0^{u_0^*} \frac{d B_v(T(u^*))}{du^*} \tau_F \left(\int_{u^*}^{u_0^*} L_v(u_1^*) du_1^* \right) du^* \quad (6)
 \end{aligned}$$

for the downward flux. Similarly, for the upward flux one finds

$$\begin{aligned}
 F_v^+(u_0^*) &\doteq B_{v,G} \tau_F \left(\int_{u_0^*}^{u^*} L_v(u_1^*) du_1^* \right) - \int_{u_0^*}^{u^*} B_v(T(u^*)) \frac{d}{du^*} \\
 &\quad \tau_F \left(\int_{u_0^*}^{u^*} L_v(u_1^*) du_1^* \right) du^* = B_v(T(u_0^*)) \\
 &\quad + \int_{u_0^*}^{u^*} \frac{d B_v(T(u^*))}{du^*} \tau_F \left(\int_{u_0^*}^{u^*} L_v(u_1^*) du_1^* \right) du^* \quad (7)
 \end{aligned}$$

In Equation (7) it is assumed that the temperature of the air directly overlying the surface of the earth equals the surface temperature.

Transforming Equations (6,7) in temperature,

$$\begin{aligned}
 F_v^+(u_0^*) &= B_v(T(u_0^*)) - B_v(T(u^*=0)) \tau_F \left(\int_0^{u_0^*} L_v(u_1^*) du_1^* \right) \\
 &\quad - \int_{T(u^*=0)}^{T(u_0^*)} \frac{d B_v(T(u^*))}{dT} \tau_F \left(\int_{u^*}^{u_0^*} L_v(u_1^*) du_1^* \right) dT \quad (8)
 \end{aligned}$$

and

$$F_v^{\uparrow}(u_0^*) = B_v(T(u_0^*)) + \int_{T(u_0^*)}^{T(u^*)} \frac{d B_v(T(u^*))}{dT} \tau_F \left(\int_{u_0^*}^{u^*} L_v(u_1^*) du_1^* \right) dT \quad (9)$$

Equations (8,9) contain some approximation but may be considered quasi-exact flux solutions. For simplicity, they will be referred to as the exact solution hereafter.

2.4 The Charlock-Herman Approximation (CH, 1976)

Equations (8,9) refer only to monochromatic radiation. Fluxes required for the wavenumber interval (v_1, v_2) are obtained from

$$F_{\Delta v}^{\uparrow}(u_0^*) = \int_{v_1}^{v_2} F_v^{\uparrow}(u_0^*) dv \quad (10)$$

and

$$F_{\Delta v}^{\uparrow}(u_0^*) = \int_{v_1}^{v_2} F_v^{\uparrow}(u_0^*) dv \quad (11)$$

The radiation table approach of EC requires that the wavenumber integration be carried out once and for all leaving the flux for a given atmospheric path a function of reduced absorbing mass only.

Inspection of Equation (5) shows that the argument of the flux

transmission function is an integral, allowing an infinite variety of atmospheric paths. Clearly, this type of situation cannot be accommodated by the simple radiation table approach which seeks to represent fluxes in the U^*T -plane. Therefore, EC introduce a measured flux transmission function defined by an expression of the form

$$\tau_F \int_{u^*}^{u_0^*} L_v(u_1^*) du_1^* = \tau_F \left\{ L_v(T(u^*)) [u_0^* - u^*] \right\}$$

$$= \tau_{F,v}(u_0^* - u^*, T(u^*)) \quad (12)$$

Equation (10) assumes that L_v is evaluated at the temperature of the elemental emitting layer instead of evaluating L_v along the entire path. This assumption is appropriate only if the temperature variation along the atmospheric path is very small (Sasamori, 1968).

CH (1976) introduce Equation (12) into Equations (8,9,10,11) and obtain

$$F_{CH}^{\downarrow}(u_0^*) = \int_{v_1}^{v_2} dv \left\{ B_v(T(u_0^*)) = B_v(T(u^*-0)) \tau_F(L_v(T(u^*=0)) u_0^*) \right.$$

$$\left. - \int_{T(u^*=0)}^{T(u_0^*)} \frac{d B_v(T(u^*))}{dT} \tau_F(L_v(T(u^*)) [u_0^* - u^*]) dT \right\} \quad (13)$$

and

$$F_{CH}^{\uparrow}(u_0^*) = \int_{v_1}^{v_2} dv \left\{ B_v(T(u_0^*)) + \frac{T(u^*)}{T(u_0^*)} \frac{d B_v(T(u^*))}{dT} \right. \\ \left. \tau_F (L_v(T(u^*)([u^* - u_0^*])dT) \right\} \quad (14)$$

2.5 The Approximation by Zdunkowski, Barth and Lombardo (1966)

Z (Charlock, Herman, Zdunkowski, 1976) looks at the problem from a different point of view. If the temperature varies considerably along the absorption path, Equation (12) may not be a sufficiently accurate approach. To account for this temperature variation a correction term $\Delta\tau_{F,v}$ should be added, i.e.,

$$\tau_F \left(\int_{u^*}^{u_0^*} L_v(T(u_1^*)) du_1^* \right) \doteq \tau_F (L_v(T(u^*)) [u_0^* - u^*]) + \Delta\tau_{F,v} \\ = \tau_F, (u_0^* - u^*, T(u^*)) + \Delta\tau_{F,v} \quad (15)$$

Due to the infinite multiplicity of absorption paths, it seems impossible to incorporate this $\Delta\tau_{F,v}$ in the radiation tables. Since an approximation like Equation (12) must be made in the radiation table approach, Z uses a partial derivative in the fundamental transfer equation, e.g.,

$$F_v^{\downarrow}(u_0^*) \doteq \int_{v_1}^{v_2} dv \left\{ B_v(T(u^*)) \frac{\partial \tau_F}{\partial u^*} (L_v(T(u^*))[u_0^* - u^*]) du^* \right\} \quad (16)$$

To approximate the temperature variation expand the partial derivative,

$$\frac{\partial \tau_{F,v}}{\partial u^*} = \frac{d\tau_{F,v}}{du^*} - \frac{\partial \tau_{F,v}}{\partial T} \frac{dT}{du^*} \quad (17)$$

Substituting Equation (17) into the up and down flux equation results in an approximate solution, used by Z, et al. (1966), of the form

$$\begin{aligned} F_Z^{\downarrow}(u_0^*) &= \int_{v_1}^{v_2} dv \left\{ B_v(T(u_0^*)) - B_v(T(u^*=0)) \tau_F(L_v(T(u^*=0))u_0^*) \right. \\ &\quad \left. - \int_{T(u^*=0)}^{T(u_0^*)} \frac{d B_v(T)}{dT} \tau_F(L_v(T)[u_0^* - u^*]) dT \right. \\ &\quad \left. - \int_{T(u^*=0)}^{T(u_0^*)} B_v(T) \frac{\partial \tau_F(L_v(T)[u_0^* - u^*])}{\partial T} dT \right\} \end{aligned} \quad (18)$$

and

$$\begin{aligned} F_Z^{\uparrow}(u_0^*) &= \int_{v_1}^{v_2} dv \left\{ B_v(T(u_0^*)) + \int_{T(u_0^*)}^{T(u^*)} \frac{d B_v(T)}{dT} \tau_F(L_v(T)[u^* - u_0^*]) dT \right. \\ &\quad \left. + \int_{T(u_0^*)}^{T(u^*)} B_v(T) \frac{\partial \tau_F(L_v(T)[u^* - u_0^*])}{\partial T} dT \right\} \end{aligned} \quad (19)$$

Comparing CH and Z approximate solutions shows

$$F_Z^{\downarrow}(u_0^*) = F_{CH}^{\downarrow}(u_0^*) - \int_{v_1}^{v_2} dv \left\{ \frac{\int_{T(u^*=0)}^{T(u_0^*)} B_v(T) \frac{\partial \tau_F(L_v(T)[u_0^*-u^*])}{\partial T} dT}{\int_{T(u_0^*)}^{T(u^*)} B_v(T) \frac{\partial \tau_F(L_v(T)[u^*-u_0^*])}{\partial T} dT} \right\} \quad (20)$$

and

$$F_Z^{\uparrow}(u_0^*) = F_{CH}^{\uparrow}(u_0^*) + \int_{v_1}^{v_2} dv \left\{ \frac{\int_{T(u^*)}^{T(u_0^*)} B_v(T) \frac{\partial \tau_F(L_v(T)[u^*-u_0^*])}{\partial T} dT}{\int_{T(u_0^*)}^{T(u^*)} B_v(T) \frac{\partial \tau_F(L_v(T)[u^*-u_0^*])}{\partial T} dT} \right\} \quad (21)$$

2.6 Numerical Treatment

The reduced absorbing mass, u^* , is calculated using trapezoidal quadrature. To obtain sufficient accuracy, u^* is determined at every 5 m for the nearest 100 meters (m) either side of the reference level and at every 25 m for the remainder of the atmosphere.

For each of the solutions (Equations 8,9,13,14,20,21) to the RTE, the monochromatic upward and downward flux through a reference level is calculated again using the trapezoidal rule. For flux calculations the nearest 100 m on either side of the reference level is divided into 25 m increments, while the remainder of the atmosphere is divided into 100 m intervals. Thus, for example, the monochromatic down flux for the exact case (Equation 8) is calculated in the following manner:

$$\begin{aligned}
 F_v^{\downarrow}(u_0^*) &= B_v(T(u_0^*)) - B_v(T(u^*=0)) \tau_F \left(\sum_{i=0}^N \left\{ \frac{1}{2}(L_{i+1} + L_i)(u_{i+1} - u_i) \right\} \right) \\
 &\quad - \sum_{i=0}^N \frac{1}{2} \left\{ \left(\frac{d B_v(i)}{dT} \tau_{F(i)} + \frac{d B_v(i+1)}{dT} \tau_{F(i+1)} \right) (T_{i+1} - T_i) \right\}
 \end{aligned} \tag{22}$$

In Equations (20,21) the partial derivative with respect to temperature is determined, as appropriate, in one of two ways. At the surface of the earth, the top of the atmosphere and at the top of an inversion a one-sided derivative approximation is used. For example,

$$\frac{\partial \tau_F}{\partial T} (L_v(T_i)[u_0^* - u_i]) \doteq \frac{\tau_F(L_v(T_{i+1})[u_0^* - u_i^*] - \tau_F(L_v(T_i)[u_0^* - u_i^*])}{T_{i+1} - T_i} \tag{23}$$

where i and $i+1$ are 10 m apart. Note that the reduced absorber mass is held constant while the temperature is allowed to vary. At all other levels in the atmosphere a centered difference scheme of the following form is used:

$$\frac{\partial \tau_F(L_v(T_i)[u_0^* - u_i^*])}{\partial T} \doteq \frac{\tau_F(L_v(T_{i+1})[u_0^* - u_i^*]) - \tau_F(L_v(T_{i-1})[u_0^* - u_i^*])}{T_{i+1} - T_{i-1}} \tag{24}$$

The slowly varying generalized absorption coefficient, L_v , is tabulated by EC for 40 cm^{-1} increments of the wavenumber spectrum for

a temperature of 293°K. For other temperatures, L_v is found from Equation (3). Since B_v and $d B_v/dT$ are virtually constant over $\Delta v = 40 \text{ cm}^{-1}$, they are evaluated at the center of the increment.

Fluxes are computed as

$$F_v(u_0^*) = \int_{v_1}^{v_2} F_v(u_0^*) \approx \sum_i^N F_i(u_0^*) \Delta v \quad (25)$$

The radiative cooling rates are proportional to the divergence of the net flux, F_N^* , i.e.,

$$\frac{dT}{dt} = \frac{-1}{\bar{p}C_p} \frac{dF_N}{dz} \approx \frac{-1}{\bar{p}C_p} \frac{\Delta F_N}{\Delta z} \quad (26)$$

where \bar{p} and C_p represent the average density of the air and the specific heat at constant pressure, respectively, and

$$F_N = F^+(z) - F^-(z) . \quad (27)$$

2.7 Properties of Approximations

In this section some qualitative statements are made which describe the two approximations. As previously stated, the important difference between the approximations and the exact solution ($F_{EX}(u_0^*)$) is the manner in which the argument of $\tau_{F,v}$ is evaluated.

First, consider the downward flux in the Atmospheric Model I (Figure 3). In the exact case one obtains

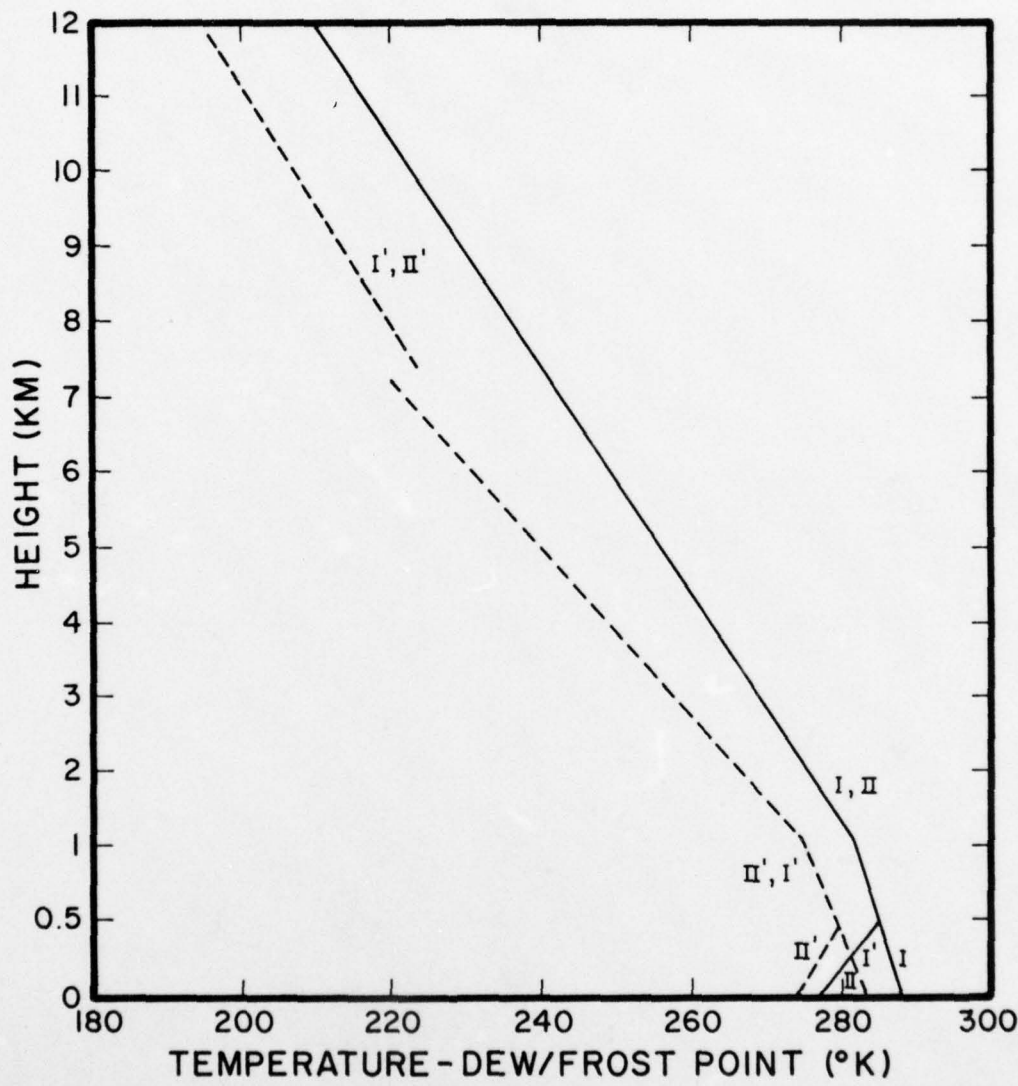


Figure 3. Model atmospheres I and II.

$$\tau_F \left(\int_{u^*}^{u_0^*} L_v(u_1^*) du_1^* \right) = \tau_F (\bar{L}_v(u_0^* - u^*)) \quad (28)$$

as follows from the mean value theorem. On the other hand, the approximate solution evaluates $\tau_{F,v}$ at the temperature of the elemental emitting layer, i.e., $\tau_F(L_v(u^*)[u_0^* - u^*])$. Since the temperature decreases with height, it is evident that (Figure 2),

$$\bar{L}_v > L_v(u^*) . \quad (29)$$

Furthermore, $\tau_{F,v}$ decreases with increasing optical pathlength thus

$$\tau_F(\bar{L}_v[u_0^* - u^*]) < \tau_F(L_v(u^*)[u_0^* - u^*]) \quad (30)$$

By comparing corresponding terms in the exact and approximate solutions for downward flux one finds from Equation (30) that

$$B_v(T(u^*=0)) \tau_F \left(\int_0^{u_0^*} L_v(T(u_1^*)) du_1^* \right) < B_v(T(u^*=0)) \tau_F(L_v(T(u^*=0) [u_0^* - 0])) \quad (31)$$

and

$$\frac{\int_{T(u^*=0)}^{T(u_0^*)} \frac{d B_v(T(u^*))}{dT} \tau_F \left(\int_{u^*}^{u_0^*} L_v(T(u_1^*)) du_1^* \right) dT}{\int_{T(u^*=0)}^{T(u_0^*)} dT} < \int_{T(u^*=0)}^{T(u_0^*)} \frac{d B_v(T(u^*))}{dT} dT$$

$$\frac{d B_v(T(u^*))}{dT} \tau_F(L_v(T(u^*))[u_0^* - u^*]) dT \quad (32)$$

Comparing Equations (8,13) it is evident that

$$F_{EX}^{\downarrow}(u_0^*) > F_{CH}^{\downarrow}(u_0^*) \quad (33)$$

for an atmosphere in which temperature decreases with height.

Still considering downward flux, given $T_2 > T_1$ it follows (Figure 2) that

$$\tau_F(L_v(T_2)[u_0^* - u^*]) - \tau_F(L_v(T_1)[u_0^* - u^*]) < 0 \quad (34)$$

and, therefore,

$$\frac{\partial \tau_F(L_v(T(u^*))[u_0^* - u^*])}{\partial T} < 0 \quad (35)$$

Hence, from Equations (13,20) it is seen that

$$F_Z^{\downarrow}(u_0^*) > F_{CH}^{\downarrow}(u_0^*) \quad (36)$$

for atmospheres of decreasing temperature with height.

Now consider briefly the upward flux for Atmospheric Model I. Analogous to the downward flux, it follows for the upward flux, from Figures 1, 2 and 3 that

$$L_v(T(u^*)) > \bar{L}_v \quad (37)$$

and

$$\tau_F(\bar{L}_v[u^* - u_0^*]) > \tau_F(L_v(T(u^*))[u^* - u_0^*]) \quad (38)$$

Therefore,

$$\begin{aligned} \int_{T(u_0^*)}^{T(u^*)} \frac{d B_v(T)}{dT} \tau_F \left(\int_{u_0^*}^{u^*} L_v(T(u_1^*)) du_1^* \right) dT &> \int_{T(u_0^*)}^{T(u^*)} \\ \frac{d B_v(T)}{dT} \tau_F(L_v(T(u^*))[u^* - u_0^*]) dT \end{aligned} \quad (39)$$

so that Equations (9,14)

$$F_{EX}^\uparrow(u_0^*) > F_{CH}^\uparrow(u_0^*) \quad (40)$$

Since $\partial \tau_{F,v} / \partial T < 0$, as in the downflux analysis, from Equations (14,21) one finds

$$F_{CH}^\uparrow(u_0^*) > F_Z^\uparrow(u_0^*) \quad (41)$$

for atmospheres with temperature decreasing with height throughout.

Next, consider the downflux in Atmospheric Model II (Figure 3). Analyzing, as earlier, the exact vs. the approximate case for the region above the top of the inversion, one finds

$$F_{EX}^\downarrow(u_0^*) > F_{CH}^\downarrow(u_0^*) \quad (42)$$

and

$$F_Z^{\uparrow}(u_0^*) > F_{CH}^{\uparrow}(u_0^*) \quad (43)$$

On the other hand, for the upward flux at reference levels below the top of the inversion, analysis, as earlier done, shows

$$\bar{L}_v > L_v(T(u^*)) \quad (44)$$

and

$$\tau_F(\bar{L}_v[u^* - u_0^*]) < \tau_F(L_v(T(u^*))[u^* - u_0^*]) \quad (45)$$

Also, since now $T_2 < T_1$, it follows that

$$\tau_F(L_v(T_2)[u^* - u_0^*]) > \tau_F(L_v(T_1)[u^* - u_0^*]) \quad (46)$$

so that

$$\frac{\partial \tau_F^* L_v(T(u^*))[u^* - u_0^*]}{\partial T} < 0 \quad (47)$$

Thus, one finds from Equations (9,14)

$$F_{EX}^{\uparrow}(u_0^*) > F_{CH}^{\uparrow}(u_0^*) \quad (48)$$

and from Equations (14,21)

$$F_Z^{\uparrow}(u_0^*) > F_{CH}^{\uparrow}(u_0^*) \quad (49)$$

III. DISCUSSION AND RESULTS

3.1 Atmospheric Models

Two model atmospheres are considered in this study. The first (i.e., I-Figure 3) is the NACA Standard Atmosphere with an assumed dewpoint distribution typical of a cloud free atmosphere. The upper level moisture profile from 7.2 to 12 KM uses a representative frost point temperature sounding (Craig, 1965). The upper and lower moisture profiles are matched in such a way as to result in a continuous function of water vapor density. The total reduced absorber mass of the atmosphere is approximately 1.2 gm cm^{-2} . The second model atmosphere (i.e., II-Figure 3) is similar to the first, but a moist inversion is introduced in the lowest 500 meters.

3.2 Flux Transmission Function

The spectral region investigated stretches from $1100-1420 \text{ cm}^{-1}$ and contains part of the vibrational-rotational water vapor band and the absorption window. In general, the flux transmission function which consists of two parts is given by

$$\tau_{F,\text{total}} = \tau_{F,\text{cont.}} \tau_{F,\text{band}} \quad (50)$$

$\tau_{F,\text{band}}$ is evaluated in terms of the generalized absorption coefficient, L_v , while the flux transmission function for the continuum is expressed in terms of the continuous absorption coefficient, k_v , i.e.,

$$\tau_{F, \text{cont}}(k_v u^*) = 2E_{i_3}(k_v u^*) \doteq e^{-1.66k_v u^*} \quad (51)$$

E_{i_3} is the exponential integral of order 3. It should be noted that k_v is multiplied by a factor of ten, as implied by EC (1960).

The flux transmission function for 6.3μ band is approximated by a piecewise cubic spline interpolant, i.e.,

$$\tau_{F,v}(x) = C_{1i} + \Delta x(C_{2i} + \Delta x(C_{3i} + \Delta x C_{4i})) \quad (52)$$

x is the optical pathlength whereas C_{1i} , C_{2i} , C_{3i} and C_{4i} are interpolant coefficients determined for each interval, i , of data points.

The quality of the fit to EC data is quite good, as verified by Table 1.

3.3 Infrared Fluxes

Upward, downward and net fluxes for Model Atmosphere I (Figure 3) are given for selected reference levels for the spectral region $1100-1420 \text{ cm}^{-1}$ in Tables 2, 3 and 4. Also shown in the Tables is the error, E , of the approximate as measured against the exact solution, i.e.,

$$E(\%) = \frac{F_{\text{approx}}(u_0^*) - F_{\text{EX}}(u_0^*)}{F_{\text{EX}}(u_0^*)} \quad (53)$$

Table 2 indicates the upward flux is generally more accurate for the CH than for the Z approximate solution. This is in agreement with

Table 1. Selected Values of Flux Transmission for Interpolant and for
 EC Data as a Function of $x = \log_{10}$ (optical path).

x	$\tau_{F,\nu}(x)$ interp	$\tau_{F,\nu}(x)$ EC
- 3.7	.99319999	.9932
- 2.9	.94390007	.9439
- 1.0	.54520075	.5452
1.0	.45000631	.45
1.1	.19000477	.19
1.2	.33751130 $\times 10^{-5}$	0

Table 2. Upward Fluxes and Approximate Solution Errors at Selected Levels for Model I.

Z(m)	F_{CH}^{\uparrow} (watts/m ²)	F_{EX}^{\uparrow} (watts/m ²)	F_Z^{\uparrow} (watts/m ²)	E_{CH} (%)	E_Z (%)
0	.45195117 x 10 ²	.45195117 x 10 ²	.45195117 x 10 ²	0	0
100	.45052779 x 10 ²	.45052887 x 10 ²	.45027406 x 10 ²	-.00	-.06
400	.44358412 x 10 ²	.44360733 x 10 ²	.44210355 x 10 ²	-.01	-.33
500	.44102414 x 10 ²	.44106115 x 10 ²	.43910295 x 10 ²	-.01	-.44
5000	.36266623 x 10 ²	.36464652 x 10 ²	.34822292 x 10 ²	-.54	-4.50
5100	.36195605 x 10 ²	.36396982 x 10 ²	.34741031 x 10 ²	-.55	-4.54
11900	.34961560 x 10 ²	.35252675 x 10 ²	.33299711 x 10 ²	-.83	-5.54
12000	.34960859 x 10 ²	.35252043 x 10 ²	.33298856 x 10 ²	-.83	-5.54

Table 3. Downward Fluxes and Approximate Solution Errors at Selected Levels for Model I.

Z(m)	F_{CH}^{\downarrow} (watts/m ²)	F_{EX}^{\downarrow} (watts/m ²)	F_Z^{\downarrow} (watts/m ²)	E_{CH} (%)	E_Z (%)
0	.22153685 $\times 10^2$.24592238 $\times 10^2$.25002371 $\times 10^2$	- 9.92	+ 1.67
100	.21359789 $\times 10^2$.23742596 $\times 10^2$.24137854 $\times 10^2$	-10.04	+ 1.67
400	.19116604 $\times 10^2$.21331968 $\times 10^2$.21679394 $\times 10^2$	-10.39	+ 1.63
500	.18416215 $\times 10^2$.20573059 $\times 10^2$.20904886 $\times 10^2$	-10.48	+ 1.61
5000	.22489071 $\times 10^1$.25224432 $\times 10^1$.25567385 $\times 10^1$	-10.84	+ 1.36
5100	.21107585 $\times 10^1$.23728110 $\times 10^1$.24007945 $\times 10^1$	-11.04	+ 1.18
11900	.70290439 $\times 10^{-6}$.70290439 $\times 10^{-6}$.70290439 $\times 10^{-6}$	0	0
12000	0	0	0	0	0

Table 4. Net Fluxes and Approximate Solution Errors at Selected Levels for Model I.

$Z(m)$	F_{N-CH} (watts/ m^2)	F_{N-EX} (watts/ m^2)	F_{N-Z} (watts/ m^2)	E_{CH} (%)	E_Z (%)
0	.23041433 $\times 10^2$.20602880 $\times 10^2$.20192746 $\times 10^{-2}$	+ 11.84	- 1.99
100	.23692990 $\times 10^2$.21310291 $\times 10^2$.20889553 $\times 10^2$	+ 11.18	- 1.97
400	.25241807 $\times 10^2$.23028765 $\times 10^2$.22530961 $\times 10^2$	+ 9.61	- 2.16
500	.25686200 $\times 10^2$.23533056 $\times 10^2$.23005410 $\times 10^2$	+ 9.15	- 2.24
5000	.34017716 $\times 10^2$.33942209 $\times 10^2$.32265554 $\times 10^2$	+ .22	- 4.94
5100	.34084847 $\times 10^2$.34024171 $\times 10^2$.32340236 $\times 10^2$	+ .18	- 4.95
11900	.34961559 $\times 10^2$.35252674 $\times 10^2$.33299711 $\times 10^2$	- .83	- 5.54
12000	.34960859 $\times 10^2$.35252043 $\times 10^2$.33298856 $\times 10^2$	- .83	- 5.54

Equations (40,41). Table 3 verifies, on the other hand, that the Z approximation yields downward fluxes generally more accurate than the CH solution. This, again, satisfies the inequalities of Equations (33,36).

Table 4 shows that the net flux error for the Z approximation is less than 6% for the selected levels chosen while the CH approximation yields maximum errors of almost 12%. The CH approximation is, however, generally more accurate in the upper levels where the downward flux is small.

For the Model II Atmosphere, as seen in Table 5, the CH approximation, again, leads to smaller upward flux errors, yet the maximum Z error is less than 3.5%. The relatively small Z errors result from more accurate fluxes in the inversion region as qualitatively expected from Equations (48,49).

Table 6 shows that, as in the Model I Atmosphere, the Z solution yields much more accurate downfluxes for Model II. The CH approximation produces errors of greater than 10% at all levels shown.

The net flux calculation for Model II are given in Table 7. Again, it is evident that the CH approximation's accuracy is best in the upper levels, while the Z solution is best in the low levels. Yet, over all levels the Z method yields a maximum error of less than 3.5%, whereas the CH method yields a maximum error of less than 15.5%.

Table 5. Upward Fluxes and Approximate Solution Errors at Selected Levels in Model II.

Z(m)	F_{CH}^{\uparrow} (watts/m ²)	F_{EX}^{\uparrow} (watts/m ²)	F_Z^{\uparrow} (watts/m ²)	E_{CH} (%)	E_Z (%)
0	.35338086 x 10 ²	.35338086 x 10 ²	.35338086 x 10 ²	0	0
100	.35568617 x 10 ²	.35569077 x 10 ²	.35609321 x 10 ²	-.00	+.11
400	.36958865 x 10 ²	.36970587 x 10 ²	.37240818 x 10 ²	-.03	+.73
500	.37563459 x 10 ²	.37583423 x 10 ²	.37954982 x 10 ²	-.05	+.99
600	.37770220 x 10 ²	.37795276 x 10 ²	.38194844 x 10 ²	-.07	+1.06
5000	.32005269 x 10 ²	.32129547 x 10 ²	.31380168 x 10 ²	-.39	-2.33
5100	.31936565 x 10 ²	.32063594 x 10 ²	.31301286 x 10 ²	-.40	-2.38
11900	.30725400 x 10 ²	.30935123 x 10 ²	.29883496 x 10 ²	-.67	-3.40
12000	.30724703 x 10 ²	.30934490 x 10 ²	.29882643 x 10 ²	-.68	-3.40

Table 6. Downward Fluxes and Approximate Solution Errors at Selected Levels in Model III.

Z(m)	F_{CH}^{\downarrow} (watts/m ²)	F_{EX}^{\downarrow} (watts/m ²)	F_Z^{\downarrow} (watts/m ²)	E_{CH} (%)	E_Z (%)
0	.18335462 $\times 10^2$.20605581 $\times 10^2$.205083940 $\times 10^2$	- 11.02	- .11
100	.18526420 $\times 10^2$.20790579 $\times 10^2$.20848291 $\times 10^2$	- 10.89	+ .28
400	.18705569 $\times 10^2$.20912403 $\times 10^2$.21194897 $\times 10^2$	- 10.55	+ 1.35
500	.18416214 $\times 10^2$.20573059 $\times 10^2$.20904888 $\times 10^2$	- 10.48	+ 1.61
600	.17737258 $\times 10^2$.19834289 $\times 10^2$.20176701 $\times 10^2$	- 10.57	+ 1.73
5000	.22489070 $\times 10^1$.25224429 $\times 10^1$.25567382 $\times 10^1$	- 10.84	+ 1.36
5100	.21107584 $\times 10^1$.23728108 $\times 10^1$.24007956 $\times 10^1$	- 11.04	+ 1.18
11900	.7029044 $\times 10^{-6}$.7029044 $\times 10^{-6}$.7029044 $\times 10^{-6}$	0	0
12000	0	0	0	0	0

Table 7. Net Fluxes and Approximate Solution Errors at Selected Levels in Model II.

Z(m)	F_{N-CH} (watts/m ²)	F_{N-EX} (watts/m ²)	F_{N-Z} (watts/m ²)	E_{CH} (%)	E_Z (%)
0	.17002624 x 10 ²	.14732505 x 10 ²	.14754146 x 10 ²	+ 15.41	+ .15
100	.17042196 x 10 ²	.14778498 x 10 ²	.14761030 x 10 ²	+ 15.32	- .12
400	.18253296 x 10 ²	.16058184 x 10 ²	.16045920 x 10 ²	+ 13.67	- .08
500	.19147246 x 10 ²	.17010364 x 10 ²	.17050094 x 10 ²	+ 12.56	+ .23
600	.20032962 x 10 ²	.17960987 x 10 ²	.18018053 x 10 ²	+ 11.54	+ .32
5000	.29756362 x 10 ²	.29607105 x 10 ²	.28823430 x 10 ²	+ .50	- 2.65
5100	.29825807 x 10 ²	.29690783 x 10 ²	.28900491 x 10 ²	+ .45	- 2.66
11900	.30725400 x 10 ²	.30935122 x 10 ²	.29883496 x 10 ²	- .67	- 3.40
12000	.30724703 x 10 ²	.30934490 x 10 ²	.29882643 x 10 ²	- .68	- 3.40

3.4 Cooling Rates

Cooling rates are computed in degrees per day for selected layers of 100 meter thickness. Table 8 indicates the cooling rates for layers centered at the heights shown for Model I. The Z cooling rates are more accurate, except at the top of the atmosphere where the heating rate is vanishingly small. Table 9 shows that the accuracy of the Z cooling rates for Model II is better than those of CH, except at the top and bottom of the atmosphere, where the cooling rates are extremely small. This suggests that the Z approximation yields more accurate flux divergence values except in regions where the divergence is vanishingly small, such as at the top of the atmosphere.

Table 8. Cooling Rates for Model I at Selected Layers

$Z(m)$	$(\frac{dT}{dt})_{EC}$ ($^{\circ}K/day$)	$(\frac{dT}{dt})_{EX}$ ($^{\circ}K/day$)	$(\frac{dT}{dt})_Z$ ($^{\circ}K/day$)	E_{CH} (%)	E_Z (%)
50	- .46140125	- .50095436	- .49344512	- 7.9	- 1.55
450	- .32683614	- .37088911	- .34894132	- 11.88	- 5.92
5150	- .07884646	- .096265721	- .087715241	- 18.09	- 8.88
11950	+ .0018643684	+ .0016805949	.0022771928	+ 10.94	+ 35.5

Table 9. Cooling Rates for Model II at Selected Layers

Z (M)	$(\frac{dT}{dt})_{CH}$ (°K/day)	$(\frac{dT}{dt})_{EX}$ (°K/day)	$(\frac{dT}{dt})_Z$ (°K/day)	E_{CH} (%)	E_Z (%)
50	- .027057626	- .031448028	- .0047069821	- 13.96	- 85.03
450	- .65482087	- .69747451	- .73556026	- 6.12	+ 5.46
550	- .6576562	- .70585053	- .71872275	- 6.83	+ 1.82
5150	- .081564298	- .098281192	- .090509416	- 17.00	- 7.91
11950	+ .0018563782	+ .0016832583	+ .002271866	+ 8.87	+ 34.96

IV. CONCLUSION

It is apparent that the CH approximation will yield more accurate upward fluxes in atmospheres of decreasing temperature with height. Equally apparent is the fact that the Z approximation produces more accurate downfluxes in such atmospheres.

The net flux through reference levels computed by the Z approximate solution seems to give a smaller error than that by CH. However, for the upper levels of an atmosphere the CH approximation, in general, yields more accurate net fluxes. If flux divergence or cooling rates are desired, it appears that the Z approximation gives better accuracy except in regions where the cooling rates are vanishingly small and likely have no real significance.

APPENDIX A

RADIATIVE TRANSFER EQUATION

To guarantee a consistent notation, it is useful to first define the following symbols:

- I_v^{\downarrow} downward intensity at wavenumber v .
- I_v^{\uparrow} upward intensity at wavenumber v .
- μ $\cos\theta$, θ is the zenith angle of the radiation
- ϕ azimuthal angle of the radiation
- J_v^{\downarrow} downward monochromatic source function
- J_v^{\uparrow} upward monochromatic source function.

A convenient and sufficient starting point is Schwartschild's Equation for downward radiation,

$$\mu \frac{dI_v^{\downarrow}(\tau, \mu, \phi)}{d\tau} = - I_v^{\downarrow}(\tau, \mu, \phi) + J_v^{\downarrow}(\tau, \mu, \phi) \quad (1)$$

and for upward radiation,

$$\mu \frac{dI_v^{\uparrow}(\tau, \mu, \phi)}{d\tau} = + I_v^{\uparrow}(\tau, \mu, \phi) - J_v^{\uparrow}(\tau, \mu, \phi) \quad (2)$$

A linear differential equation of the form,

$$\frac{dy}{dx} + P(x) y(x) + Q(x) = 0 \quad (3)$$

has the following solution

$$y(x) = e^{-\int_{x_0}^x P(z)dz} [y(x_0) - \int_{x_0}^x Q(t) e^{\int_{x_0}^t P(z)dz} dt]. \quad (4)$$

Thus, from Equations (1,2) one finds

$$I_v^{\uparrow}(\tau, \mu, \phi) = I_v^{\uparrow}(\tau_1, \mu, \phi) \exp(-(\tau_1 - \tau)/\mu) + \int_{\tau}^{\tau_1} J_v^{\uparrow}(t, \mu, \phi) \exp(-(t - \tau)/\mu) \frac{dt}{\mu} \quad (5)$$

for upward intensity and

$$I_v^{\downarrow}(\tau, \mu, \phi) = I_v^{\downarrow}(0, \mu, \phi) \exp(-\tau/\mu) + \int_0^{\tau} J_v^{\downarrow}(t, \mu, \phi) \exp(-(\tau - t)/\mu) \frac{dt}{\mu} \quad (6)$$

for downward intensity where from Figure 4,

$$\tau_v = \int_0^{u_0} K_v(u_1) du_1 \equiv \text{optical pathlength for the reference level} \quad (7)$$

$$\tau_v = \int_0^u K_v(u_1) du_1 \equiv \text{optical path for an arbitrary level} \quad (8)$$

$$\tau_{1v} = \int_0^U K_v(u_1) du_1 \equiv \text{total optical path for the atmosphere} \quad (9)$$

See Figures 1,4. Under the Black Body assumption the infrared intensity is defined by the Plank function

$$I_v(\mu, \phi) = B_v / \pi \quad (10)$$

Therefore, the radiation fluxes, as obtained from the intensity by angular integration,

$$F_v(\tau) = \int_0^{2\pi} \int_0^1 I_v(\tau, \mu) \mu d\mu = 2 \int_0^1 B_v \mu d\mu \quad (11)$$

Transforming Equations (5,6) using Equations (10,11) yields the monochromatic flux equations. Assuming the radiation at the top of the atmosphere is zero, the monochromatic downward flux at a reference level is

$$F_v^{\downarrow}(\tau_v) = 2 \int_0^{\tau_v} \int_0^1 B_v(t_v) \exp \left\{ -\frac{1}{\mu} (\tau_v - t_v) \right\} \mu d\mu \frac{dt}{\mu} \quad (12)$$

The monochromatic upward flux at the reference level is

$$F_v^{\uparrow}(\tau_v) = 2 B_{v,G} \int_0^1 \exp \left\{ -\frac{1}{\mu} (\tau_{1v} - \tau_v) \right\} \mu d\mu + 2 \int_{\tau_v}^{\tau_{1v}} B_v(t_v) \int_0^1 \exp \left\{ -\frac{1}{\mu} (t_v - \tau_v) \right\} \mu d\mu \frac{dt}{\mu} \quad (13)$$

Differentiating Equation (8) with respect to the upper limit yields

$$dt_v = K_v(u) du \quad (14)$$

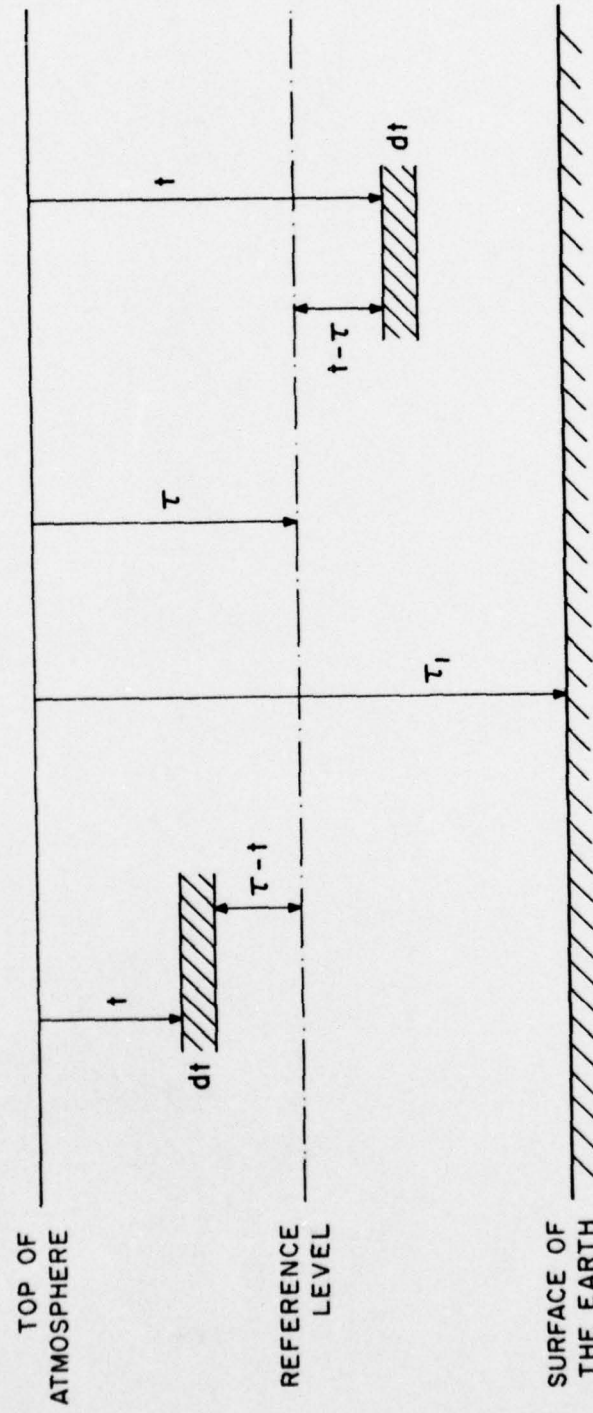


Figure 4. Schematic representation of optical path for flux integration.

Also,

$$\tau_v - t_v = \int_0^{u_0} K_v(u_1) du_1 - \int_0^u K_v(u_1) du_1 = \int_u^{u_0} K_v(u_1) du_1 \quad (15)$$

Substituting Equations (14,15) into Equations (12,13) gives, for the downward flux at a reference level,

$$F_v^{\downarrow}(u_0) = 2 \int_0^{u_0} B_v(u) \int_0^1 \exp \left\{ -\frac{1}{\mu} \int_u^{u_0} K_v(u_1) du_1 \right\} d\mu K_v(u) du \quad (16)$$

and for the upward flux,

$$F_v^{\uparrow}(u_0) = 2B_{v,G} \int_0^1 \exp \left\{ -\frac{1}{\mu} \int_{u_0}^u K_v(u_1) du_1 \right\} d\mu K_v(u) du$$

$$+ 2 \int_{u_0}^u B_v(u) \int_0^1 \exp \left\{ -\frac{1}{\mu} \int_{u_0}^u K_v(u_1) du_1 \right\} d\mu K_v(u) du \quad (17)$$

It is advantageous at this point to eliminate the integration over μ . Recall

$$1/\mu = \sec \theta \equiv \xi \text{ then } d\xi = \sec \theta \tan \theta d\theta \text{ and } d\mu = -\sin \theta d\theta.$$

Let

$$x = \int_u^{u_0} K_v(u_1) du_1 \quad (18)$$

Then

$$2 \int_0^1 \exp \left\{ -\frac{1}{\mu} \int_u^{u_0} K_v(u_1) du_1 \right\} d\mu = 2 \int_0^{\pi/2} \exp \{-\sec \theta\} \sin \theta d\theta = 2 \int_1^\infty \exp(-x\xi) \frac{d\xi}{\xi^2}. \quad (19)$$

Introducing the exponential integral,

$$E_{i_n}(x) = \int_1^\infty \exp(-x) \frac{d\xi}{\xi^2} \quad (20)$$

produces

$$2 \int_0^1 \exp \left\{ -\frac{1}{\mu} \int_u^{u_0} K_v(u_1) du_1 \right\} u du = 2E_{i_2} \left(\int_u^{u_0} K_v(u_1) du_1 \right) \quad (21)$$

The derivative of the exponential integral is defined as

$$\frac{dE_{i_n}(x)}{dx} = -E_{i_{n-1}}(x) \quad (22)$$

Thus it is evident that

$$-E_{i_2}(x) = \frac{dE_{i_3}(x)}{du} \frac{du}{dx} \quad (23)$$

But

$$\frac{du}{dx} = 1/\left(\frac{dx}{du}\right) = 1/\left(\frac{d}{du} \int_u^{u_0} K_v(u_1) du_1\right) = -\frac{1}{K_v(u)} \quad (24)$$

Substituting Equation (24) into Equation (23) and rearranging yields

$$K_v(u) E_{i_2}(x) = \frac{dE_{i_3}(x)}{du} \quad (25)$$

Now as is customary define the flux transmission function

$$\tau_{F,v} = 2E_{i_3}(x) \quad (26)$$

From Equations (21,25,26) and Equations (16,17) one finds for the downward flux at a reference level

$$F_v^{\downarrow}(u_0) = \int_0^{u_0} B_v(u) \frac{d}{du} \{ \tau_{F,v} \left(\int_u^{u_0} K_v(u_1) du_1 \right) \} du \quad (27)$$

Similarly, for the upward direction at a reference level,

$$F_v^{\uparrow}(u_0) = B_{v,G} \tau_{F,v} \left(\int_{u_0}^U K_v(u_1) du_1 \right) - \int_{u_0}^U B_v(u) \frac{d}{du} \{ \tau_{F,v} \left(\int_{u_0}^u K_v(u_1) du_1 \right) \} du \quad (28)$$

BEST AVAILABLE COPY

APPENDIX B

LISTINGS OF COMPUTER PROGRAMS

Spline Interpolant Program

```
1#      ' DIMENSION XI(50),C(4,50),X3(197),Y(197),NP(1),A1(5),A2(5),A3(5)
2#      DATA (A1(I),I=1,5)/* CUBIC SPLINE INTERPOLANT   */
3#      DATA (A2(I),I=1,5)/*                           X          */
4#      DATA (A3(I),I=1,5)/*                           FX         */
5#      NP(1)=197
6#      READ (5,500)N1
7#      500 FORMAT(I2)
8#      READ(5,501) (XI(I),C(1,I),I=1,N1)
9#      C(2,1)=C(1,1)*(2.*XI(1)-XI(2)-XI(3))/((XI(1)-XI(2))*(XI(1)-XI(3)))
10*     +*(XI(2)-XI(3))/((XI(2)-XI(1))*(XI(2)-XI(3)))
11*     +*(C(1,3)*(XI(1)-XI(2))/((XI(3)-XI(1))*(XI(3)-XI(2)))
12*     C(2,N1)=C(1,N1-2)*(XI(N1)-XI(N1-1))/((XI(N1-2)-XI(N1-1))*(XI(N1-2)
13*     -XI(N1)))+C(1,N1-1)*(XI(N1)-XI(N1-2))/((XI(N1-1)-XI(N1-2))*(
14*     1(XI(N1-1)-XI(N1)))+C(1,N1)*(2.*XI(N1)-XI(N1-2)-XI(N1-1))/(
15*     1(XI(N1)-XI(N1-2))*(XI(N1)-XI(N1-1)))
16*     N=N1-1
17*     CALL SPLINE(N,XI,C)
18*     CALL CALCCF(N,XI,C)
19*     501 FORMAT(2F5.2)
20*     X=XI(1)
21*     DO 10 J=1,197
22*     X3(J)=X

23*     FX=PCUBIC(X,N,XI,C)
24*     Y(J)=FX
25*     WRITE(6,600) J,X,FX
26*     600 FORMAT(15,F10.5,E20.9)
27*     10 X=X+.025
28*     DO 601 I=1,N1
29*     WRITE(7,601) C(2,I),C(3,I),C(4,I)
30*     601 FORMAT(3E15.9)
31*     601 FORMAT(3E15.9)
32*     CALL IUPLOT(12..12.)
33*     CALL EZPLOT(X3,Y,1,NP,1,1,A1,A2,A3)
34*     CALL FINI
35*     STOP
END
```

BEST AVAILABLE COPY

43

Spline Program (continued)

```
1*      SUBROUTINE SPLINE(N,XI,C)
2*      DIMENSION XI(50),C(4,50),D(50),DIAG(50)
3*      DATA 1/1.0/
4*      NP1=N+1
5*      DO 10 M=2,NP1
6*      U(M)=XI(M)-XI(M-1)
7*      10 DIAG(M)=(C(1,M)-C(1,M-1))/U(M)
8*      DO 20 M=2,N
9*      C(2,M)=3.* (D(M)+DIAG(M+1))+D(M+1)*DIAG(M)
10*     20 DIAG(M)=2.* (U(M)+D(M+1))
11*     DO 30 M=2,N
12*     G=-U(M+1)/DIAG(M-1)
13*     DIAG(M)=DIAG(M)+G*U(M-1)
14*     30 C(2,M)=C(2,M)+G*C(2,M-1)
15*     NJ=NP1
16*     DO 40 M=2,N
17*     NJ=M-1
18*     40 C(2,NJ)=(C(2,NJ)-D(NJ)*C(2,NJ+1))/DIAG(NJ)
19*     RETURN
20*     END
```

```
1*      SUBROUTINE CALCCF(N,XI,C)
2*      DIMENSION XI(50),C(4,50)
3*      DO 10 I=1,N
4*      DX=XI(I+1)-XI(I)
5*      DIVDF1=(C(1,I+1)-C(1,I))/DX
6*      DIVDF3=C(2,I)+C(2,I+1)-2.*DIVDF1
7*      C(3,I)=(DIVDF1-C(2,I)-DIVDF3)/DX
8*      10 C(4,I)=DIVDF3/DX/DX
9*      RETURN
10*     END

1*      FUNCTION PCUBIC(XBAR,N,XI,C)
2*      DIMENSION XI(50),C(4,50)
3*      DATA 1/1/
4*      UX=XBAR-XI(1)
5*      IF (UX) 10,30,20
6*      10 IF (I.EQ.1) GO TO 30
7*      I=I-1
8*      UX=XBAR-XI(I)
9*      IF (UX) 10,30,30
10*     19 I=I+1
11*     UX=UX
12*     20 IF (2.EQ.N) GO TO 30
13*     DDX=XBAR-XI(I+1)
14*     IF (DDX) 30,19,19
15*     30 PCUBIC=C(1,I)+UX*(C(2,I)+DX*(C(3,I)+DX*C(4,I)))
16*     RETURN
17*     END
```

BEST AVAILABLE COPY

Flux Program for Model II

```

1*      DIMENSION II(900),TZ(900),XI(50),C(4,50),GLZ(900)
2*      N=50
3*      READ(5,500) (C(2,I),C(3,I),C(4,I),C(1,I),XI(I),I=1,N)
4*      500 FORMAT(5E15.9)
5*      502 READ(5,501,END=999)ZRL,V,GL0,CON
6*      501 FORMAT(F6.0,F5.0,F5.2,E12.8)
7*      DZ=12000.0-ZRL
8*      MD=UZ/100.
9*      MU=MD-1
10*     MU=ZRL/100.
11*     MU=MU-1
12*     ZD2=12000.
13*     Z2=ZD2
14*     L=1
15*     U(1)=0.
16*     TZ(1)=T(ZD2)
17*     GLZ(1)=GL(TZ(1),V,GL0)
18*     C COMPUTES U* AT EACH LEVEL
19*     IF(MD.LT.0) U0=0.
20*     IF(MD.LT.0) TO=T(ZD2)
21*     IF(MD.LT.0) GO TO 8
22*     IF(MD.EQ.0) GO TO 9
23*     DO 1 I=1,MD
24*     DO 2 J=1,4
25*     L=L+1
26*     Z1=Z2-25.
27*     TZ(L)=T(Z1)
28*     GLZ(L)=GL(TZ(L),V,GL0)
29*     UU=.5*(PH0(22)*(P(Z2)/1013.)*((293./T(Z2))**(.5))+RHO(Z1)*(P(Z1)/
30*     11013.)*((293./T(Z1))**(.5)))*(Z2-Z1)*100.
31*     U(L)=U(L-1)+UU
32*     Z2=Z1
33*     2 CONTINUE
34*     1 CONTINUE
35*     C COMPUTES U* FOR INTERVAL 100 M ABOVE REFERENCE LEVEL TO 100 M BELOW
36*     Z2=ZRL+100.
37*     9 DO 3 I=1,5

```

BEST AVAILABLE COPY

```

38*      DO 4 J=1*4
39*      L=L+1
40*      Z1=Z2-5.
41*      TZ(L)=T(Z1)
42*      GLZ(L)=GL(TZ(L),V, GLO)
43*      UU=.5*(RHO(Z2)*(P(Z2)/1013.)*(1293./T(Z2))**(.5)+RHO(Z1)*(P(Z1)/
44*      11013.)*(1293./T(Z1))**(.5)))*(22-Z1)*100.
45*      U(L)=U(L-1)+UU
46*      Z2=Z1
47*      4 CONTINUE
48*      3 CONTINUE
49*      U0=U(L)
50*      T0=TZ(L)
51*      IF(MU.LT.0) GO TO 11
52*      8 DO 7 I=1*5
53*      0010 J=1*4
54*      L=L+1
55*      Z1=Z2-5.
56*      TZ(L)=T(Z1)
57*      GLZ(L)=GL(TZ(L),V, GLO)
58*      UU=.5*(RHO(Z2)*(P(Z2)/1013.)*(1293./T(Z2))**(.5)+RHO(Z1)*(P(Z1)/
59*      11013.)*(1293./T(Z1))**(.5)))*(22-Z1)*100.
60*      U(L)=U(L-1)+UU
61*      Z2=Z1
62*      10 CONTINUE
63*      7 CONTINUE
64*      C COMPUTES U* FOR REMAINING LEVELS DOWN TO THE SURFACE
65*      Z2=ZRL-100.
66*      IF(MU.EQ.0) GO TO 11
67*      00 5 I=1*MJ
68*      DO 6 J=1*4
69*      L=L+1
70*      Z1=Z2-25.
71*      TZ(L)=T(Z1)
72*      GLZ(L)=GL(TZ(L),V, GLO)
73*      UU=.5*(RHO(Z2)*(P(Z2)/1013.)*(1293./T(Z2))**(.5)+RHO(Z1)*(P(Z1)/
74*      11013.)*(1293./T(Z1))**(.5)))*(22-Z1)*100.
75*      U(L)=U(L-1)+UU
76*      Z2=Z1
77*      6 CONTINUE
78*      5 CONTINUE
79*      C COMPUTES U* AT THE SURFACE(UG)
80*      UG=U(L)
81*      C COMPUTES THE DOWN FLUX AT THE REFERENCE LEVEL FOR CH AND Z METHODS
82*      11 IFLAG=1
83*      J=1
84*      IF(MD.LT.0) DFTC=0.
85*      IF(MD.LT.0) DFTZ=0.
86*      IF(MD.LT.0) GO TO 104
87*      TS=T2(1)
88*      UL=GL(TS,V, GLO)+ALOG10(U0)
89*      IF(V.GT.1200.) CON=0.
90*      TRCON=EXP(-16.6*CON*U0)
91*      TRX=PCUPIC(UL,1)*TRCON
92*      DFB=BETA(T0,V)-BETA(TZ(1),V)*TPX
93*      GLI=GL(TS,V, GLO)
94*      EO=BETA(T0,V)

```

BEST AVAILABLE COPY

```

95*      BI=BETA(TZ(1),V)
96*      WRITE(6,604)UL,TRX,DFB
97*      WRITE(6,620)U0,GL1,B0,BI,DFB
98*      620 FORMAT(5(E15.8))
99*      604 FORMAT(1X,3(E16.8))
100*      DFIC=0.
101*      DFZ=0.
102*      T2=TZ(1)
103*      IF(ND,NE,0) GO TO 112
104*      TRII=TRX
105*      DB2=DB(T2,V)
106*      B2=BETA(T2,V)
107*      DTR2=DTR(T2,U0,N,ZD2,V,GLO,ZRL,CON)
108*      GO TO 103
109*      112 DO 100 M=1,10
110*      J=J+4
111*      ZD1=ZD2-10n.
112*      T1=TZ(J)
113*      U1=U0-U(J)
114*      IF(N,GT,1) GO TO 105
115*      TRII=TRX
116*      DTR2=DTR(T2,U0,N,ZD2,V,GLO,ZRL,CON)
117*      DB2=DB(T2,V)
118*      B2=BETA(T2,V)
119*      105 UL1=GLZ(J)+ ALOG10(U1)
120*      TRCOM1=EXP(-16.6*CON*U1)
121*      TRI=TRCOM1*PCUBIC(UL1,N)
122*      B1=BETA(T1,V)
123*      DB1=DB(T1,V)
124*      DF=.5*(DB2*TRII+DR1*TRI)*(T1-T2)
125*      DFIC=DFI+DF
126*      107 DTR1=DTR(T1,U1,N,ZD1,V,GLO,ZRL,CON)
127*      DDF2=.5*(B2*DTR2+R1*DTR1)*(T1-T2)
128*      DFZ=DFZ +DDF2
129*      ZD2=ZD1
130*      WRITE(6,698)J,DTR1,TRI,DDF2,DF,ZD1,U1,GLZ(J),UL1,CON
131*      698 FORMAT(1X,I3,8(E14.8),1X,E12.8)
132*      TRII=TRI
133*      DB2=DB1
134*      B2=B1
135*      DTR2=DTR1
136*      100 T2=T1
137*      103 DO 101 M=1,5
138*      J=J+4
139*      ZD1=ZD2-20.
140*      T1=TZ(J)
141*      U1=U0-U(J)
142*      106 IF(U1,LE,0.) GO TO 102
143*      UL1=GLZ(J)+ ALOG10(U1)
144*      GO TO 109
145*      102 UL1=-3.8
146*      109 TRCOM1=EXP(-16.6*CON*U1)
147*      TRI=TRCOM1*PCUBIC(UL1,N)
148*      DR1=DB(T1,V)
149*      DF=.5*(DB2*TRII+DR1*TRI)*(T1-T2)
150*      JJ2=J-4
151*      DFIC=DFIC+DF

```

BEST AVAILABLE COPY

```

152*      B1=BETA(T1,V)
153*      108 UTR1=DTR(T1,U1+N,ZD1,V,GLO,ZRL,IFLAG)
154*      DDFZ=.5*(B2*CTR2+R1*DTR1)*(T1-T2)
155*      DFZ=DFZ+DDFZ
156*      WRITE(6,698)J,DTR1,TRI,DFZ,DF,ZD1,U1,GLZ(J),UL1,CON
157*      IF(J.LT.460,OR,J.GT.477) GO TO 110
158*      WRITE(6,602)J,ZD2,T2,CON,TRII,DTR2,DF
159*      WRITE(6,602)J,DFIC,DB2,DB1,B2,R1,DFZ
160*      WRITE(6,602)J,ZD1,T1,UL1,GLZ(J),TRI,DTR1
161*      WRITE(6,603)J,U(J),U(J-4),GLZ(J-4)
162*      602 FORMAT(1X,T3,6(1X,E16.8))
163*      603 FORMAT(1X,T3,3(E16.8))
164*      110 TRII=TRI
165*      B2=B1
166*      DB2=DB1
167*      DTR2=DTR1
168*      T2=T1
169*      101 ZD2=ZD1
170*      DFTC=DFB-DFC
171*      DFTZ=DFB-DFC-DFZ
172*      C COMPUTES THE UP FLUX AT THE FEERENCE LEVEL FOR THE CH AND Z CASES
173*      104 UFIC=0.
174*      UFZ=0.
175*      IFLAG=2
176*      UFB=BETA(T0      ,V)
177*      IF(MU.LT.0) GO TO 205
178*      C COMPUTES THE UPFLUX FOR THE LAYER FROM THE REFERENCE LEVEL TO 100 M BELOW
179*      DO 200 M=1,5
180*      J=J+4
181*      ZD1=ZD2-20.
182*      T1=TZ(J)
183*      U1=U(J)-U0
184*      IF(M.GT.1) GO TO 206
185*      TRII=1.
186*      T2=TZ(J-4)
187*      DB2=DB(T2,V)
188*      B2=BETA(T2,V)
189*      DTR2=0.
190*      206 UL1=GLZ(J)+ALOG10(U1)
191*      TRCONI=EXP(-16.6*CON*U1)
192*      TRI=TRCONI*PCUBIC(UL1,N)
193*      DB1=DB(T1,V)
194*      UF=.5*(DB2*TRII+DB1*TRI)*(T1-T2)
195*      UFIC=UFIC+UF
196*      U1=BETA(T1,V)
197*      207 DTR1=DTR(T1,U1+N,ZD1,V,GLO,ZRL,CON)
198*      UUFZ=.5*(B2*DTR2+R1*DTR1)*(T1-T2)
199*      UFZ=UFZ+UUFZ
200*      JJ2=J-4
201*      WRITE(6,698)J,DTR1,TRI,UUFZ,UF,ZD1,U1,GLZ(J),UL1,CON
202*      IF(J.LT.478,OR,J.GT.485) GO TO 211
203*      WRITE(6,602)J,ZD2,T2,CON,TRII,DTR2,UF
204*      WRITE(6,602)J,UFIC,DB2,DB1,B2,B1,UFZ
205*      WRITE(6,602)J,ZD1,T1,UL1,GLZ(J),TRI,DTR1
206*      WRITE(6,603)J,U(J),U(J-4),GLZ(J-4)
207*      211 TRII=TRI
208*      DB2=DB1

```

BEST AVAILABLE COPY

```

209*      B2=B1
210*      DTR2=DTR1
211*      T2=T1
212*      200 ZD2=ZD1
213*      C COMPUTES THE UP FLUX FOR THE LAYER FROM 100 M BELOW THE REFERENCE LEVEL TO THE
214*      C SURFACE
215*      IF(MU,EQ.0) GO TO 205
216*      DO 201 M=1,MU
217*      ZD1=ZD2-100.
218*      J=J+4
219*      T1=T2(J)
220*      U1=U(J)-U0
221*      ULI=GLZ(J)+ALOG10(U1)
222*      DB1=DB(T1,V)
223*      TRCONI=EXP(-16.6*CON*U1)
224*      TRI=TRCONI*PCUBIC(ULI,N)
225*      209 UFF=.5*(DB2*TRI+DB1*TRI)*(T1-T2)
226*      UFIC=UFIC+UF
227*      B1=BETA(T1,V)
228*      210 DTR1=DTR(T1,U1,N,ZD1,V,GLO,ZRL,CON)
229*      UUFZ=.5*(B2+DTR2*R1*DTR1)*(T1-T2)
230*      UFZ=UUFZ+UUFZ
231*      WRITE(6,608)J,DTR1,TRI,UUFZ,UF,ZD1,U1,GLZ(J),UL1,CON
232*      TRII=TRI
233*      DB2=DB1
234*      B2=U1
235*      DTR2=DTR1
236*      T2=T1
237*      201 ZD2=ZD1
238*      205 UFTC=UFG+UFIC
239*      UFTZ=UFR+UFIC+UFZ
240*      C COMPUTES THE DOWN FLUX AT THE REFERENCE LEVEL FOR THE EXACT CASE
241*      204 II=1
242*      K=1
243*      IF(MD,LT,0) DFTE=0.
244*      IF(MD,LT,0) GO TO 303
245*      ULE=ALOG10(SUM(K,MD,II,M,IFLAG))
246*      TRCONE=EXP(-16.6*CON*U0)
247*      TRE=TRCONE*PCUBIC(ULE,N)
248*      DFBET=BETA(T0,V)-BETA(TZ(1),V)*TRE
249*      WRITE(6,604)ULE,TRE,DFBE
250*      DFIE=0.
251*      T2=TZ(1)
252*      C COMPUTES THE DOWN FLUX FOR THE LAYER FROM THE TOP OF THE ATM TO 100 M ABOVE
253*      C THE REFERENCE LEVEL
254*      IF(MD,NE,0) GO TO 308
255*      TRII=TRE
256*      DB2=DB(T2,V)
257*      GO TO 302
258*      308 DO 300 M=1,MD
259*      I2=M+1
260*      K=K+4
261*      T1=TZ(K)
262*      IF(M,GT,1) GO TO 306
263*      TRII=TRE
264*      DB2=DB(T2,V)
265*      306 UL1=ALOG10(SUM(K,MD,I2,M,IFLAG))

```

BEST AVAILABLE COPY

```

266*      U1=U0-U(K)
267*      DB1=DB(T1,V)
268*      TRCON1=EXP(-16.6*CON*U1)
269*      TRI=TRCON1*PCUBIC(UL1,N)
270*      DFE=.5*(DB2*TRI1+DB1*TRI)*(T1-T2)
271*      DFIE=DFIE+DFE
272*      WRITE(6,660)K,TRI,DFE,UL1,U1,DB1,DFIE
273*      TRII=TRI
274*      DB2=DB1
275*      300 T2=T1
276*      302 IFLAG=3
277*      C COMPUTES THE DOWN FLUX FOR THE LAYER FROM 100 M ABOVE THE REFERENCE LEVEL
278*      C TO THE REFERENCE LEVEL
279*      DO 301 M=1,5
280*      K=K+4
281*      T1=TZ(K)
282*      M2=M+1
283*      U1=U0-U(K)
284*      307 IF(M2.LE.5) GO TO 309
285*      UL1=-3.8
286*      U1=0.
287*      GO TO 305
288*      309 UL1=ALOG10(SUM(K,MD,M,M2,IFLAG))
289*      305 DB1=DB(T1,V)
290*      TRCON1=EXP(-16.6*CON*U1)
291*      TRI=TRCON1*PCUBIC(UL1,N)
292*      DFE=.5*(DB2*TRI1+DB1*TRI)*(T1-T2)
293*      DFIE=DFIE+DFE
294*      KK2=K-4
295*      WRITE(6,660)K,TRI,DFE,UL1,U1,DB1,DFIE
296*      IF(K,LT,469,OR,K.GT,477)GO TO 304
297*      WRITE(6,602)K,T2,CON,TRII,DFIE,DFBE,DFE
298*      WRITE(6,603)K,DB1,DB2,DFIE
299*      WRITE(6,603)KK2,T1,UL1,TRI
300*      304 DB2=DB1
301*      TRII=TRI
302*      301 T2=T1
303*      DFTE=DFBE-DFIE
304*      C COMPUTES THE UP FLUX AT THE REFERENCE LEVEL FOR THE EXACT CASE
305*      303 UFIE=0.
306*      UFBE=BETA(T0,V)
307*      IF(MU,LT,0) GO TO 403
308*      C COMPUTES THE UPFLUX FOR THE LAYER FROM THE REFERENCE LEVEL TO 100 M BELOW
309*      DO 400 M=1,5
310*      K=K+4
311*      T1=TZ(K)
312*      U1=U(K)-U0
313*      IF(M,GT,1) GO TO 404
314*      TRII=1.
315*      T2=TZ(K-4)
316*      DB2=DB(T2,V)
317*      404 UL1=ALOG10(SUMU(K,MU,M,M,IFLAG))
318*      DB1=DB(T1,V)
319*      TRCON1=EXP(-16.6*CON*U1)
320*      TRI=TRCON1*PCUHIC(UL1,N)
321*      UFEE=.5*(DB2*TRI1+DB1*TRI)*(T1-T2)
322*      UFIE=UFIE+UFE

```

BEST AVAILABLE COPY

```

323*      KK2=K-4
324*      WRITE(6,660)K,TRI,UFF,UL1,U1,DB1,UFFE
325*      660 FORMAT(1X,I3,6E15.8)
326*      IF(K.LT.478.OR.K.GT.485) GO TO 407
327*      WRITE(6,602)K,TRII,UFFE,UFFE,DB1,DB2
328*      WRITE(6,603)KK2,T1,UL1,TRI
329*      407 TRII=TRI
330*      DB2=DB1
331*      400 T2=T1
332*      IF(MU.EQ.0) GO TO 403
333*      C COMPUTES THE UPFLUX FOR THE LAYER FROM 100 M BELOW THE REFERENCE LEVEL TO THE
334*      C SURFACE
335*      IFLAG=4
336*      DO 401 M=1,MU
337*      K=K+4
338*      T1=TZ(K)
339*      406 UL1=ALOG10(SUMU(K,MU,M,N,IFLAG))
340*      U1=U(K)-U0
341*      DB1=DB(T1,V)
342*      TRCONI=EXP(-16.6*CON*U1)
343*      TRI=TRCONI*PCUBIC(UL1,N)
344*      405 UFFE=.5*(DB2*TRII+DB1*TRI)*(T1-T2)
345*      UFFE=UFFE+UFFE
346*      WRITE(6,660)K,TRI,UFFE,UL1,U1,DB1,UFFE
347*      TRII=TRI
348*      DB2=DB1
349*      401 T2=T1
350*      403 UFTE=UFFE+UFTB
351*      402 WRITE(6,601)
352*      601 FORMAT(1X,6X,'DFTC',10X,'DFTE',10X,'DFTZ',10X,'UFTC',13X,'UFTE',
353*      110X,'UFTZ')
354*      WRITE(6,600) DFTC,DFTE,DFTZ,UFTC,UFTE,UFTZ,GLO,V,ZRL,TO
355*      600 FORMAT (6(1X,E14.9),4F8.2)
356*      GO TO 502
357*      999 STOP
358*
359*      FUNCTION SUM(K2,M1,I1,J1,IFLAG)
360*      SUM1=0.
361*      KS=K2
362*      IF(IFLAG.EQ.3) GO TO 6
363*      IF(I1.GT.M1) GO TO 10
364*      11 DO 2 IS=I1,M1
365*      DO 3 JS=1,4
366*      KS=KS+1
367*      A2=10.*GLZ(KS)
368*      A1=10.*GLZ(KS)
369*      S=.5*(A2+A1)*( U(KS)-U(KS-1))
370*      SUM1=SUM1+S
371*      3 SUM=SUM1
372*      2 CONTINUE
373*      10 JI=1
374*      6 DO 4 IS=JI,5
375*      8 DO 5 JS=1,4
376*      KS=KS+1
377*      A2=10.*GLZ(KS-1)
378*      A1=10.*GLZ(KS)
379*      S=.5*(A2+A1)*( U(KS)-U(KS-1))

```

BEST AVAILABLE COPY

```

380*      SUM1=SUM1+S
381*      IF(K2.LT.469.OR.K2.GT.477) GO TO 5
382*      WRITE(6,650)KS,GLZ(KS-1),GLZ(KS)*A2,A1,S,SUM1
383*      650 FORMAT(1X,T3,6(E15.8))
384*      5 SUM=SUM1
385*      4 CONTINUE
386*      9 RETURN
387*
388*      FUNCTION SUMU(K3,M3,I3,J3,IFLAG)
389*      SUM2=0.
390*      KU=K3
391*      IF(IFLAG.EQ.4) GO TO 4
392*      DO 2 IU=1,J3
393*      DO 3 JU=1*4
394*      KU=KU-1
395*      A1=10.*GLZ(KU+1)
396*      A2=10.*GLZ(KU)
397*      S=.5*(A2+A1)*(U(KU+1)-U(KU))
398*      SUM2=SUM2+S
399*      IF(K3.LT.478.OR.K3.GT.485) GO TO 3
400*      WRITE(6,650)KU,GLZ(KU+1),GLZ(KU)*A2,A1,S,SUM2
401*      650 FORMAT(1X,T3,6(E15.8))
402*      WRITE(6,655)U(KU+1),U(KU)
403*      655 FORMAT(1X,2E15.8)
404*      3 SUMU=SUM2
405*      IF(J3.EQ.5) SUM3=SUMU
406*      2 CONTINUE
407*      RETURN
408*      4 SUM2=SUM3
409*      DO 5 IU=1,I3
410*      DO 6 JU=1*4
411*      KU=KU-1
412*      A1=10.*GLZ(KU+1)
413*      A2=10.*GLZ(KU)
414*      S=.5*(A2+A1)*(U(KU+1)-U(KU))
415*      SUM2=SUM2+S
416*      6 SUMU=SUM2
417*      5 CONTINUE
418*      RETURN
419*
420*      FUNCTION PCUBIC(XBAR,N)
421*      I=1
422*      IF(XBAR.LT.-3.7) PCUBIC=1.
423*      IF(XBAR.LT.-3.7) RETURN
424*      IF(XBAR.GT.1.2) PCUBIC=0.
425*      IF(XBAR.GT.1.2) RETURN
426*      DX=XBAR-XI(I)
427*      IF(DX) 10,30,20
428*      10 IF(I.EQ.1) GO TO 30
429*      I=I-1
430*      DX=XBAR-XI(I)
431*      IF(DX) 10,30,30
432*      19 I=I+1
433*      DX=DX
434*      20 IF(2.EQ.N) GO TO 30
435*      DX=XBAR-XI(I+1)
436*      IF(DX) 30,19,19

```

BEST AVAILABLE COPY

```

437*      30 PBIC =C(1,I)+DX*(C(2,I)+DX*(C(3,I)+DX*C(4,I)))
438*      PCUBIC=PBIC*.01
439*      RETURN
440*
441*      FUNCTION RHO(Z)
442*      IF (Z-7200..GE.0.) GO TO 1
443*      XX=5422.99*((1./273.)-(1./TD(Z)))+ALOG(6.11)
444*      E=(EXP(XX))*1000.
445*      RHO=E/(.461*(10.**7.)*T(Z))
446*      RETURN
447*      1 XXX=6147.5054*((1./273.)-(1./TD(Z)))+ALOG(6.11)
448*      E=(EXP(XXX))*1000.
449*      RHO=E/(.461*(10.**7.)*T(Z))
450*      RETURN
451*
452*      FUNCTION T(Z)
453*      IF(Z-500..GE.0.) GO TO 1
454*      T=277.+(7.75/500.)*Z
455*      RETURN
456*      1 T=288.-.0065*Z
457*      RETURN
458*
459*      FUNCTION TD(Z)
460*      IF(Z-500..GE.0.) GO TO 1
461*      TD=274.+(6./500.)*Z
462*      RETURN
463*      1 IF(Z-7200..GE.0.) GO TO 2
464*      TU=279.-(5A. /6700)*(Z-500.)
465*      RETURN
466*      2 TD=T(Z)-15.
467*      RETURN
468*
469*      FUNCTION P(Z)
470*      IF(Z-10769..GE.0.) GO TO 1
471*      P=((Z/-44308.)+1.)**(1./.19023))*1013.25
472*      RETURN
473*      1 P=234.52/EXP((Z-10769.)/6381.6)
474*      RETURN
475*
476*      FUNCTION GL(TT,V,GL0)
477*      IF(V-1595..GT.0.) GO TO 1
478*      A=2.4/(10.**5.)
479*      GO TO 2
480*      1 A=1.75/(10.**5.)
481*      2 B=2.22
482*      GL=GL0-A*((293.-TT)/TT)*((V-1595.)**2.)*ALOG10(293./TT)
483*      RETURN
484*
485*      FUNCTION BETA(TT,V)
486*      PB=3.7411676/(10.**12.)
487*      Q=1.4389
488*      BETA=(PB*(V**3.))/((EXP(Q*V/TT)-1.))
489*      RETURN
490*
491*      FUNCTION Dn(TT,V)
492*      PB=3.7411676/(10.**12.)
493*      Q=1.4389

```

BEST AVAILABLE COPY

53

```
494* DB=((((PB*(TT**2.))/(0**3.))*(Q*V/TT)**4.)*EXP(Q*V/TT))/((EXP(Q*V
495* 1/TT)-1.)*2.)
496* RETURN
497*
498* FUNCTION DTR(TT,UZ,N,ZZ,V,GL0,ZRL,CON)
499* KZ=ZZ-11990.
500* IF(KZ.GT.0) GO TO 1
501* JZ=ZZ-10.
502* IF(JZ.LT.0) GO TO 2
503* IZ=ZZ-500.
504* IF(IZ.LT.-10.AND.IZ.GE.0) GO TO 2
505* IF(IZ.LT.0.AND.IZ.GE.-10) GO TO 1
506* ZZ1=ZZ+10.
507* ZZ3=ZZ-10.
508* TT1=T(ZZ1)
509* TT2=TT
510* TT3=T(ZZ3)
511* IF(UZ.LE.0.) DTR=0.
512* IF(UZ.LE.0.) GO TO 3
513* UT1=GL(TT1,V,GL0)+ALOG10(UZ)
514* UT3=GL(TT3,V,GL0)+ALOG10(UZ)
515* TCON=EXP(-16.6*CON*UZ)
516* TR1=PCURIC(UT1,N)*TCON
517* TR3=PCURIC(UT3,N)*TCON
518* DTR=(TR3-TR1)/(TT3-TT1)
519* GO TO 3
520* 1 TT1=TT
521* ZZ2=ZZ-10.
522* TT2=T(ZZ2)
523* IF(UZ.LE.0.) DTR=0.
524* IF(UZ.LE.0.) GO TO 3
525* UT1=GL(TT1,V,GL0)+ALOG10(UZ)
526* UT2=GL(TT2,V,GL0)+ALOG10(UZ)
527* TCON=EXP(-16.6*CON*UZ)
528* TR1=PCURIC(UT1,N)*TCON
529* TR2=PCURIC(UT2,N)*TCON
530* DTR=(TR2-TR1)/(TT2-TT1)
531* GO TO 3
532* 2 TT3=TT
533* ZZ2=ZZ+10.
534* TT2=T(ZZ2)
535* IF(UZ.LE.0.) DTR=0.
536* IF(UZ.LE.0.) GO TO 3
537* UT2=GL(TT2,V,GL0)+ALOG10(UZ)
538* UT3=GL(TT3,V,GL0)+ALOG10(UZ)
539* TCON=EXP(-16.6*CON*UZ)
540* TR2=PCURIC(UT2,N)*TCON
541* TR3=PCURIC(UT3,N)*TCON
542* DTR=(TR3-TR2)/(TT3-TT2)
543* GO TO 3
544* 3 IF(ZZ.GT.560..OR.ZZ.LT.460.) GO TO 40
545* WRITE(6,660)TT1,TT2,TC0',UT1,UT2,UT3,UZ
546* WRITE(6,660)TR1,TR2,TR3,TT1,TT2,TT3,DTR
547* 660 FORMAT(1X,7(E15.8))
548* 40 RETURN
549* END
```

BEST AVAILABLE COPY

54

Interpolant Coefficient Input

c_{2i}	c_{3i}	c_{4i}	c_{1i}	x_i
-.290016556+01	-.491083684+01	-.875228740+00	.993190997+02	-.369999999+01
-.390859014+01	-.517346756+01	.259348184+01	.987499995+02	-.359999999+01
-.466546719+01	-.439534655+01	.500619464+00	.985400000+02	-.350000000+01
-.572952167+01	-.424510371+01	.540337622+01	.980100002+02	-.340000001+01
-.641645736+01	-.262417254+01	-.211244717+01	.973929996+02	-.330000001+01
-.700466549+01	-.325791193+01	.30608378+01	.967249995+02	-.319999999+01
-.756486535+01	-.234408331+01	-.724077309+01	.960000000+02	-.309999999+01
-.803585422+01	-.236580741+01	-.275647670+01	.952200003+02	-.300000000+01
-.859170997+01	-.319274801+01	.109808457+01	.94390003+02	-.290000001+01
-.919731712+01	-.286332658+01	.163459699+01	.935000000+02	-.280000001+01
-.991902051+01	-.335371393+01	.456132936+01	.925500002+02	-.269999999+01
-.106266032+02	-.472212577+01	-.118136420+00	.915299997+02	-.259999999+01
-.115745726+02	-.475758100+01	-.496764632+01	.904200001+02	-.250000000+01
-.126751002+02	-.624770558+01	-.129222884+01	.892100000+02	-.240000001+01
-.139250269+02	-.625158751+01	-.494689552+01	.879800001+02	-.230000001+01
-.153247737+02	-.774566951+01	-.637654507+01	.864200001+02	-.219999999+01
-.168758563+02	-.776498636+01	-.476479584+01	.848100004+02	-.209999999+01
-.185718002+02	-.913444132+01	-.875473119+00	.830400000+02	-.200000000+01
-.204369528+02	-.945769617+01	-.173387495+01	.810900002+02	-.190000001+01
-.223803687+02	-.997726727+01	-.218873048+01	.786949998+02	-.180000000+01
-.244415640+02	-.106338968+02	.490379240+00	.766099997+02	-.170000000+01
-.265535724+02	-.104367917+02	.224781051+00	.740600004+02	-.159999999+01
-.28641872+02	-.104193693+02	-.178802543+01	.713000020+02	-.150000000+01
-.307637020+02	-.106357991+02	.532817739+01	.683299999+02	-.140000001+01
-.327770166+02	-.923733759+01	.749568097+01	.651499996+02	-.130000000+01
-.346222353+02	-.921486294+01	.437230989+01	.617800002+02	-.120000000+01
-.363340327+02	-.790318531+01	.243549374+01	.582300000+02	-.109999999+01
-.378416114+02	-.717254096+01	.588703042+01	.545200000+02	-.100000000+01
-.390995693+02	-.540645111+01	.401544553+01	.506700001+02	-.899999999+00
-.400603356+02	-.420181299+01	.805149162+01	.467100000+02	-.799999997+00
-.406591939+02	-.178642270+01	.377979269+01	.426700001+02	-.700000003+00
-.409030447+02	-.652503952+00	.682945222+00	.385900002+02	-.600000001+00
-.408286624+02	.139c28884+01	.890350306+01	.345000000+02	-.500000000+00
-.42823000+02	.406731135+01	.75562021+01	.304400001+02	-.399999999+00
-.392421331+02	.633433507+01	.109698840+02	.264600000+02	-.300000001+00
-.376491660+02	.959527969+01	.896425247+01	.226099999+02	-.199999999+00
-.354611655+02	.122345697+02	.132727623+02	.189500000+02	-.999999996+01
-.326060686+02	.162664032+02	.794491768+01	.155400000+02	.000000000+00
-.291144007+02	.186498618+02	.494742393+01	.124500000+02	.999999946+01
-.252360659+02	.201340742+02	.226583472+01	.97300002+01	.199999999+00
-.211412759+02	.208138266+02	-.401067746+01	.741000003+01	.300000001+00
-.170988324+02	.196106143+02	-.622291539+01	.550000000+01	.399999999+00
-.133633972+02	.177437301+02	-.110975493+02	.397999999+01	.500000000+00
-.10475778+02	.144146628+02	-.928682520+01	.281000000+01	.600000001+00
-.754628998+01	.115904100+02	-.113551329+02	.193000001+01	.700000003+00
-.556726229+01	.819136305+01	-.519239879+01	.128000000+01	.799999997+00
-.403466160+01	.66314661+01	-.757522043+01	.799999997+00	.899999999+00
-.219449605+01	.427157217+01	-.339672876+01	.449999999+00	.100000000+01
-.223n97752+01	.32795246+01	.110224465+01	.189999999+00	.100000000+01
-.154999985+01	.000000000	.000000000	.000000000	.120000000+01

BEST AVAILABLE COPY

55

Model I Functions

```

451*      FUNCTION T(Z)
452*      1 T=286.-.0065*Z
453*      RETURN
454*
455*      FUNCTION TD(Z)
456*      1 IF(Z>7200.+GE.0.) GO TO 2
457*      TD=283.3283E-(58./6700.)*Z
458*      RETURN
459*      2 TD=T(Z)-15.
460*      RETURN
461*

492*      FUNCTION DTR(UZ,V,ZZ,V,GL0,Z,RL,COM)
493*      KZ=ZZ-11090.
494*      IF(KZ.GT.0.) GO TO 1

495*      JZ=ZZ-10.
496*      IF(JZ.LT.0.) GO TO 2
497*      ZZ1=ZZ+10.
498*      ZZ3=ZZ-10.
499*      TT1=T(ZZ1)
500*      TT2=TT
501*      TT3=T(ZZ3)
502*      IF(UZ.LE.0.) DTR=0.
503*      IF(UZ.LE.0.) GO TO 3
504*      UT1=GL(TT1,V,GL0)+ALOG10(UZ)
505*      UT3=GL(TT3,V,GL0)+ALOG10(UZ)
506*      TCON=EXP(-16.6*COM*UZ)
507*      TR1=PCUBIC(UT1,1)*TCON
508*      TR3=PCUBIC(UT3,1)*TCON
509*      DTR =(TR3-TR1)/(TT3-TT1)
510*      GO TO 3
511*      1 TT1=TT
512*      ZZ2=ZZ-10.
513*      TT2=T(ZZ2)
514*      IF(UZ.LE.0.) DTR=0.
515*      IF(UZ.LE.0.) GO TO 3
516*      UT1=GL(TT1,V,GL0)+ALOG10(UZ)
517*      UT2=GL(TT2,V,GL0)+ALOG10(UZ)
518*      TCON=EXP(-16.6*COM*UZ)
519*      TR1=PCUBIC(UT1,1)*TCON
520*      TR2=PCUBIC(UT2,1)*TCON
521*      DTR =(TR2-TR1)/(TT2-TT1)
522*      GO TO 3
523*      2 TT3=TT
524*      ZZ2=ZZ+10.
525*      TT2=T(ZZ2)
526*      IF(UZ.LE.0.) DTR=0.
527*      IF(UZ.LE.0.) GO TO 3
528*      UT2=GL(TT2,V,GL0)+ALOG10(UZ)
529*      UT3=GL(TT3,V,GL0)+ALOG10(UZ)
530*      TCON=EXP(-16.6*COM*UZ)
531*      TR2=PCUBIC(UT2,1)*TCON
532*      TR3=PCUBIC(UT3,1)*TCON
533*      DTR =(TR3-TR2)/(TT3-TT2)
534*      GO TO 3
535*      3 IF(ZZ.GT.560..OR.ZZ.LT.460.) GO TO 40
536*      WRITE(6,660) TT1,TT2,TCON,UT1,UT2,UT3,UZ
537*      WRITE(6,660) TR1,TR2,TR3,TT1,TT2,TT3,DTR
538*      660 FORMAT(1Y,7(E15.8))
539*      "0 RETURN
540*      END

```

REFERENCES

Charlock, T., B. M. Herman and W. G. Zdunkowski, 1976: Comments on "Discussion of the Elsasser formulation for infrared fluxes." J. Appl. Meteor., 15, 1317-1319.

Charlock, T. and B. M. Herman, 1976: Discussion of the Elsasser formulation for infrared fluxes. J. Appl. Meteor., 15, 657-661.

Conte, S. D. and C. deBoor, 1972: Elementary Numerical Analysis: An Algorithmic Approach. New York, McGraw-Hill Company, pp. 233-240.

Craig, R. A., 1965: The Upper Atmosphere: Meteorology and Physics. New York, Academic Press, pp. 34-37.

Elsasser, W. M. and M. F. Culbertson, 1960: Atmospheric radiation tables. Meteor. Monogr., No. 23, 44 pp.

Kourganoff, V., 1952: Basic Methods in Transfer Problems. Oxford, Oxford University Press, 281 pp.

Sasamori, T., 1968: The radiative cooling calculation for application to general circulation experiments. J. Appl. Meteor., 7, 721-729.

Zdunkowski, W. G., 1971: On radiation tables of Elsasser and Culbertson. J. Appl. Meteor., 10, 174.

_____, R. E. Barth and F. A. Lombardo, 1966: Discussion on the atmospheric radiation tables by Elsasser and Culbertson. Pure Appl. Geophys., 63, 211-219.

VITA

Name	Paul Joseph Breslin Captain, United States Air Force
Birthdate	October 6, 1948
Birthplace	Ft. Bragg, North Carolina
High School	Pallotti High Laurel, Maryland
University	University of Maryland College Park, Maryland 1966-1971
	North Carolina State University Raleigh, North Carolina 1972-1973 Basic Meteorology Training
Degree	B.S. Aerospace Engineering 1971
Honorary Societies	Chi Epsilon Pi

